Pedo-geochemical background and sediment contamination of metal(loid)s in the old mining-district of Salsigne (Orbiel valley, France)

Gauthier Delplace, Jérôme Viers, Eva Schreck, Priscia Oliva, Philippe Behra

Pedo-geochemical background and sediment contamination of metal(loid)s in the old mining-district of Salsigne (Orbiel valley, France)

Gauthier Delplace [a], Jérôme Viers [a,*], Eva Schreck [a], Priscia Oliva [a], Philippe Behra [b]

[a] Géosciences Environnement Toulouse (GET), Université de Toulouse, CNRS, IRD 14 Avenue Edouard Belin, 31400, Toulouse, France

[b] Laboratoire de Chimie Agro-industrielle, LCA, Université de Toulouse, INRAE, 31030 Toulouse, France

[*] Corresponding author. Email address: jerome.viers@get.omp.eu (J. Viers)

Abstract

The mining district of Salsigne in the Orbiel valley (Aude, France) was at one time the first gold mine in Europe and the first arsenic mine in the world. However, no scientific studies have evaluated the magnitude of its environmental impact. In this study, the pedo-geochemical background (PGB) was determined for 14 metal(loid) elements, including As. It appears that the PGB values for As and Sb are relatively high with 44 ±12 and 0.9 ± 1.2 mg.kg^{-1}, respectively, because of the geological particularities of this area. In a second step, these PGB values (normalized with Ti concentrations) were used as local references to determine enrichment factors (EFs) of bed river sediments for the Orbiel River and two of its major tributaries (Gresillou and Russec rivers) collected between November, 2018 and July, 2020. Results showed that riverine sediments are contaminated by past mining activity and/or current storage areas. If we except the major elements (Fe, Ti and at a lesser extent Mn), we observed that As, Cu, Sb, Pb present the highest concentrations relative to the remaining elements (Cd, Co, V, Ni and Cr). In the case of As, EFs can reach 74 in the Orbiel River, 1000 in the Gresillou River and 27 in the Russec River. These calculations were also performed for sediments transported by the extreme flood of October 14, 2018, that killed 15 people and potentially remobilized contamination in the valley. We

observed that the As concentrations of suspended samples from Grésillou and Russec rivers have reached 870 $mg.kg^{-1}$.

Finally, the As concentrations measured in the river sediments of this valley are of the same order of magnitude than those published in the literature for environments strongly impacted by mining or mineral processing activities.

Keywords

Arsenic, metal(loid)s, Orbiel valley, environmental contamination, geochemical background, soil, mines

1. Introduction

Mining and ore processing activities during the so-called modern period (19th and 20th centuries) have strongly impacted the natural environments by releasing metals, metalloids as well as other products used in industrial processes (e.g., cyanide, polyacrylamide) everywhere in the world. These released compounds have a strong impact on the Critical Zone, but also on human health through food (solid and liquid) ingestion, absorption through skin, and air inhalation (Plumlee and Ziegler, 2007; Landrigan et al., 2018; Li et al., 2021). Together with the manufacturing industry, mining activities have played (and are playing) a major role in the dispersion of metals and metalloids through environment compartments, i.e. surface and ground waters, soils/sediments, atmosphere and biosphere (Purves, 1985; Nriagu et Pacyna, 1988). Face to these legacies of the past and before to carry out rehabilitation, it is necessary to establish rigorous contamination diagnostics, based on the specific study of each environmental compartment. The first compartment to be considered is the source reservoir, which corresponds to soils and sediments that have witnessed primary contamination from mining activities (Salomons and Förstner, 1984; Resongles et al., 2014). In order to assess the level of contamination of soils and sediments, it is necessary - first of all - to know the geochemical background of the area of interest in order to used it as a local reference.

Our work fits in this general context and more particularly in the Orbiel valley (South France) context, where was located the Salsigne mining district corresponding at one time to the largest gold mine in Europe and the largest arsenic mine in the world (Pujol, 2014). Following the closure of the mine in 2004, some rehabilitation has been undertaken. Nevertheless, recent works published by Khaska et al. (2015, 2018) have shown that As concentrations in surface (Orbiel River) and ground waters were high (36-40 $\mu g.L^{-1}$) downstream the remediated zone whereas the upstream concentrations were in the 2-6 $\mu g.L^{-1}$ range. During flood, the As concentrations measured in the Orbiel River may be significantly higher (~120 $\mu g.L^{-1}$ during the flood of May 22, 2012). These authors have explained

these high concentrations by the contribution of anthropogenic arsenic (Ca-arsenate). If these publications have revealed a strong contribution of old mining sites on the waters of the valley, no scientific studies have been published to give an overview of the contamination of soils or sediments in this valley. However, in October 2018, the potential contamination of arsenic and other metal(loid)s in this valley resurfaced with force following the extreme flash flood of the Orbiel River. Dramatic consequences have occurred on local populations (loss of 15 human lives, destroyed infrastructures), together with remobilization and dispersion of contaminants, which may have some strong environmental impacts (Girardeau, 2019; Lebouc et al., 2019). Even if this extreme hydroclimatic event has recently awaken the attention of authorities and local populations, this area has been poorly studied in the past as previously highlighted, and especially regarding the environmental consequences of the mining activities and the potential risks involved for human health. Indeed, because of its physical and chemical properties, As can induce serious health problems in humans (Duker et al., 2005; Bulka et al., 2016; Saint-Jacques et al., 2018).

The main objectives of this study were then: i) to define the pedogeochemical background (PGB) on the basis of a rigorous methodology; and ii) to use this prerequisite estimated PGB to assess the level of sediment contamination of the Orbiel River and of its major tributaries. Different soils, which were sampled from various geological formations located uphill of the mining district, in pristine environments, were analyzed. The PGB was then determined for 14 metal(oïd)s, and compared to data available at national and European scales. Sediments were collected in various rivers in this mining district. Their metal(loid)s contents were determined and discussed according to the PGB determined in the first part.

This work constitutes an indispensable and fundamental preliminary study to be able to address in the near future the problems of exposure and risks for the populations living in these contaminated environments.

2. Material and methods

2.1 Site description

2.1.1 *Geological context*

The Orbiel valley is located on the southern slope of the Montagne Noire, the south-western terminus of the Massif Central (France) (Figure 1). It consists first of a central nucleus of granites and gneiss, surrounded by a halo of micaschists (Tollon, 1970; Berger et al., 1993; Cassard et al., 1993). These micaschists form a metasedimentary cover varying in age from Cambro-Ordovician to Devonian (Cassard et al., 1993). Further south, the southern slope of the Montagne Noire is composed predominantly of Palaeozoic carbonate formations, strongly folded and dislocated, and thrust sheet dating from the Hercynian orogenesis (Cassard et al., 1993). Finally, a Tertiary cover in total discordance with the Hercynian base can be observed in the south. This Tertiary cover presents in its northern part mainly limestone and in its southern part fluvial sedimentary deposits ("Carcassonne 's molasse").

The studied zone contains the Salsigne district, a major Au deposit that belong to the Variscan gold province. Mineralization processes (i.e., hydrothermal) occurred during late orogenic processes between 330 and 290 Ma and have affected late Proterozoic to early Cambrian schists, early Cambrian sedimentary rocks, Devonian limestones and sandstone (Bouchot et al., 2005). Indeed, many metalliferous bodies have been identified in the area, as evidenced by past mining activities (and particularly the second Age of Iron, the Roman period, and the modern period of the 19^{th} and 20^{th} centuries) (Fabre et al., 2016). These bodies can be classified in filonian and stratiform bodies, according to Tollon (1970). The "metalliferous district of Salsigne", which is rich in arsenic, gold, lead and bismuth, is located in the southern slope of the Montagne Noire. The most represented mineral phases in the deposits are sulphide, such as pyrite (FeS_2), arsenopyrite (FeAsS), pyrrhotite ($Fe_{1-x}S$ where $0 < x < 0.2$), chalcopyrite ($CuFeS_2$) and bismuthinite (Bi_2S_3); and to a lesser extent galena (PbS),

sphalerite ((Zn,Fe)S), scheelite ($CaWO_4$) and wolframite ($(Fe,Mn,Mg)WO_4$) (Marcoux and Lescuyer, 1994; Demange et al., 1986).

2.1.2 *Historic context of mining exploitation and waste storage*

During the modern mining period, the mining district of Salsigne included various concessions: Malabau, Pujol, Lastours, La Caunette, Salsigne, Villanière, and Villardonnel (Geoderis, 2012). These concessions are reported in Figure 1 with the main sites that have been exploited for extraction and/or treatment in the past and the main current waste deposits. It has been estimated that nearly 12 million t of ore would have been extracted to produce around 120 t of gold, and 450,000 t of arsenic during the period 1873-2004 (Girard, 2011). About 15,000 t of copper were also produced, as well as silver (~150 t) and bismuth (~800 t).

During the last period of mining activity (1992-1997), the SEPS company (Société d'Exploitation et de Pyrométallurgie de Salsigne) has also reprocessed foreign waste from the area mine using the powerful water jacket furnace, inherited from the pyrometallurgical process of ore treatment. This company has also played a major role in the dispersion of contaminants in the environment. Nowadays, the main waste storage areas are located at Montredon (4 million t of waste rock containing 10 to 12% arsenic), Artus (7 million t of waste rock), and La Combe du Saut. The Montredon storage area contains mainly waste from the cyanuration of the ore, but also flotation residues, lime arsenates, residues from the Malabau mine, and sewage sludge; La Combe du Saut mainly contains waste from the demolition of the plant and buildings (furnace crucibles, bricks, drums, etc.), from the SEPS company and pyrometallurgic slag (Desaulty et al., 2016). A lime arsenate storage area is also located at La Combe du Saut, close to the Orbiel bedriver. It comes from the water treatment plant that recoils percolation water from the Montredon and Artus sites. This water treatment plant extracts most of the arsenic from these waters by precipitating lime arsenites ($Ca_3(AsO_4)$) before their released in the Orbiel

River. Unlike Montredon, the storage of the Artus is neither sealed in the background nor covered by an impermeable system. The seepage water thus passes through the 10 Million t of tailings by progressively loading with arsenic, cyanides and other chemical elements.

2.1.3 *Hydrological context*

The Orbiel valley has a typically continental climate with both Mediterranean and oceanic influences, with relatively high annual rainfall (900 mm), a relatively mild average temperature (13 °C) and frequent winds (>300 days/yr). The source of the Orbiel River is in the Montagne Noire at 900 m in elevation close to the city of Labruguière (Tarn, France). About 40 km long, it flows in a southern direction to reach the Aude River in the Trèbes town, east of Carcassonne (Figure 2). The Orbiel River has a watershed of approximately 250 km^2 and three major tributaries (Russec, Rieutord and Clamoux). Another tributary is the intermittent Gresillou River (Figure 2). At Bouilhonnac, the Orbiel River has an average annual flow of 2.67 $m^3.s^{-1}$ (http://hydro.eaufrance.fr/). Due to the Mediterranean influence, this catchment is regularly affected by high and extreme flash flood events during which maximum flows can reach several hundreds of $m^3.s^{-1}$ (e.g. 450 $m^3.s^{-1}$ during the flood of 14-15 October 2018; Lebouc et al., 2019). The Orbiel River flowing from north to south crosses the former mining district of Salsigne. The Russec River drains: (*i)* the former concessions of Villardonel and Malabau, particularly La Messette site; (*ii)* the western area of the former open-pit mine of Salsigne drained by the Gourg Peyris River, a left bank tributary of the Russec River; and (*iii)* and the western flank of the Montredon storage site. The Gresillou River drains the waste Ramèle and Nartau deposits.

Apart from the former mining activity and its legacies (abandoned mines, waste storage areas, etc.), there are no other significant activities in this watershed. From an economic point of view the two main activities are tourism and viticulture. However, this tourist activity is limited (mainly hiker) with very little impact on the natural environment and the vineyard is relatively small with little influence on our area of study. The urbanized places are the villages that we can meet along the Orbiel River, in the

section we studied (Miraval-Cabardes, Mas Cabardes, Les Ilhes, Lastours). These villages have a population varying between 50 and 190 inhabitants. There is no urbanized area on the Gresillou and Russec rivers.

2.2 Soils sampling strategy

Because the Orbiel valley presents a strong variability in terms of lithology (Figure 1), we collected a representative soil sample set for each major geological formation outcropping uphill of the mining district, in relatively pristine zones. To this end, old and recent satellites pictures, ancient pre-industrial mine maps (Fabre et al., 2016) and maps of tailing location (Figure 2) were used to select pristine sampling sites. Forest soils were privileged as sampling sites, as the presence of trees ensure that soils were not, or almost not, disturbed, at least for the lifetime of the existent trees (Horckmans et al., 2005). Some sampling were performed in moorlands with the presence of shrubs, when forests were absent or unreachable. Totally, seven sites, labelled in accordance with the label given in the geological map for their parental rock, were sampled uphill of the mining district (Spd, Spe, Spf, Spg, Sph, Spi, Srk) for the pedo-geochemical background determination, and two sites were sampled within the district (k1 and k2b) for elemental contents comparison (Figure 1).

The sampling methodology for soils in each selected site was derived from the one used in the French RMQS program (Jolivet et al., 2016). For each site, the methodology was based on a composite sampling at different depth coupled with a soil profile description. Thus, a soil pit was dug in order to describe the soil profile morphology and estimate succession and depths of main horizons in order to define the composite sampling depths. Then, composite samples were formed, following a square grid pattern of (10 m × 10 m) divided into 16 sub areas. For each horizon, or every 20 cm when the horizon was too thick, 16 sub-samples were taken randomly in each sub area (homogeneously distributed within the square), and bulked together. The sampling was conducted until the substratum or the saprolite (C horizon), which was sampled as well, was reached. Sampled were taken using a soil auger

(Edelman Ø 7 cm), which was cleaned with demineralized water between each composite sampling depth, kept in hermetic plastic bags, which were immediately labelled. Back to the laboratory, they were oven dried for a week at 50 °C, sieved at 2 mm using a nylon sieve, and crushed in an agate mortar prior to mineralization. The soils morpho-genetic description (from field study) was reported in the supplementary material (SM-1) for each geological formation and sampling site.

2.3 Sediment sampling

All the sediments were collected during several sampling campaigns: 11/12/2018, 12/14/2018, 01/17/2019, 04/16-17/2019, and 07/21/2020. Sediments were sampled directly in or the closest to the riverbed, and stored in clean, new, 50 mL polycarbonate tubes. Back to the laboratory, they were oven dried for a week at 50 °C and crushed in an agate mortar prior to mineralization.

Sediments were sampled in 12 locations along the three main streams in the valley: the Orbiel River, and **two of its** tributaries, the Grésillou and the Russec rivers (Figure 2). The Orbiel River was sampled at Miraval-Cabardès (called MIR), in the upstream portion, and going downstream at Mas-Cabardès (MAS), at Lastours (LAS) before the confluence with the Gresillou River, at Moulin d'Artigues (ART), at Pont de Limousis (LIM), and finally at Gué de Lassac (GUE); the Gresillou River was sampled upstream (NAU) and downstream the storage area of Nartau (NAD); the Russec River was sampled at Raissac (RAI), Salitis (SLT) and St-Angel (ANG); all these three sites are located downstream close to the confluence with Orbiel River.

In this work, we took into account two other types of solid samples: (i) samples collected in November and December 2018, corresponding to precipitates (labelled GUE-2 and GUE-3) formed within an excavation created in the plain bordering the Orbiel River, at the station Gué de Lassac by the flash flood, on October 14-15, 2018; and (ii) sediments, named LAG-1, ANG-1, ANG-2, ANG-3 and ANG-4, for which we are sure that they were deposited during the extreme flash flood, on October 14-15, 2018. During this flood, no water sampling (and suspended sediment) could be collected due to the

violence of the event. However, when the average speed of the river decreases, deposits of sediments occurred on flooded surfaces. The suspended particulate matter considered in this work are sediments that have been deposited on certain surfaces and that we were able to recover after the flood. Sediments denoted LAG-1 correspond to Grésillou suspended sediments deposited in the schoolyard of Lastours, sampled in April 2019. From the Russec River, sediments ANG-1 and ANG-3 were sampled at the same location, in November 2018 and January 2019, respectively, and corresponds to suspended sediments deposited as mud on a field. These samples were collected near the confluence between Russec and Orbiel rivers, and could be considered as samples representing a mixture of suspended sediments from both rivers. ANG-2 and ANG-4 are suspended sediments from the Russec River deposited in an empty wine tank, and in the warehouse storage of the farm at the Wine Castle Saint Angel, respectively.

2.4 Determination of elemental concentrations

Elemental concentrations in soil samples were determined after acid digestion of 50 mg of dried soil or sediment. This procedure was performed using a Millestone® Ultrawave microwave at the HSM laboratory (HydroSciences Montpellier, France) in a class 10,000 clean room. Firstly, 1 mL HF (40%, Merck Suprapur), 3 mL HNO_3 (67-69%, Analytika Analpure), and 3 mL HCl (30%, Merck Suprapur), were added together in closed Teflon vials containing 50 mg of sample. Then, the acid digestion was performed in the microwave, where samples were heated for 5 min at 100 °C, then 5 min at 150 °C, and finally 5 min at 200 °C, at a pressure starting at 40 bar (N_2) and increasing to 80-100 bar. Blank tests indicated that the level of contamination induced by the acid digestion procedure was negligible, < 2% of the less concentrated element. Samples were then let to evaporate to dryness on a hotplate and then diluted with 3 mL 1% HNO_3 and put in an ultrasound bath for 20 min. Finally, they were heated on a hotplate at 100 °C for 10 min. A certified reference material, “Montana II Soil” (NIST-SRM 2711a, Mackey et al., 2010), underwent the same procedure.

Samples were then analyzed using ICP-MS (iCAP Q, Thermo Scientific- Kinetic Energy Discrimination mode using He) at the AETE-ISO platform (OSU OREME/Université de Montpellier, France). Metal(loid) concentrations were determined with external calibration using (Be, Sc, Ge, Rh, Ir) as internal standards to correct potential sensitivity drifts. Limits of quantification were: (i) lower than 1 µg.kg^{-1} for Cd, Co, Cr, Ni, Pb, Sb, U and V; (ii) between 1 and 3 µg.kg^{-1} for As, Mn, Ti and Zn; (iii) 35 µg.kg^{-1} for Cu; and (iv) 121 µg.kg^{-1} for Fe. Uncertainties associated to the measurement were inferior to 3%. The agreement of certified sample analysis with certified concentrations was better than 85% for Cr, Pb and Ti, and 95% for As, Cd, Co, Cu, Fe, Mn, Ni, Sb, U, V, Zn.

2.5 Enrichment factor (EF) and Geoaccumulation index determination

EF were determined using the following relationship:

$$EF = \left(\frac{[X]}{[Ti]}\right)_Y \Big/ \left(\frac{[X]}{[Ti]}\right)_Z \quad \text{(Eq. 1)}$$

For soil EF calculation, with respect to national or international references, Y = PGB data and Z = reference data. For sediment EF calculation, Y = sediment data and Z = PGB data. Ti concentration was chosen as reference in order to erase pedological variations and anomalies due to natural pedogenitic processes, external sources or anthropogenic activities. An EF close to 1 indicates an absence of contamination while a value significantly greater than 1 indicates a contribution by an anthropogenic source.

Considering the high lithological variability from upstream to downstream, it was difficult, if not impossible, to define a natural geochemical background for sediments. We could have defined this sediment geochemical background in the uppermost part of the watershed, but considering this variability of lithology, would it have been representative of sediments all along the stream? We believe that no. Therefore, using the PGB as a reference for sediments was a much more robust process for us.

Geo-accumulation index (Igeo) have been calculated for sediments according to the formula proposed by Müller (1969):

$$Igeo = \log2 (C_{sed} / 1.5\ C_{ref}) \quad \text{(Eq. 2)}$$

where C_{sed} is the element concentration in the sediment and C_{ref} the element concentration in the reference, PGB for us here. Müller (1969) proposed several classes to define sediment quality: 0: uncontaminated; between 0 and 1: uncontaminated to moderately contaminated; between 1 and 2: moderately contaminated; between 2 and 3: moderately to strongly contaminated; between 3 and 4: strongly contaminated; between 4 and 5: strongly to extremely contaminated; above 5: extremely contaminated.

2.6 Statistical analyses for soil data treatment

Two Kruskal-Wallis tests were performed using PAST 4.01® software, in order to assess significant differences between: (i) surface horizon and substratum (C horizon), and (ii) between soils sampled uphill of the mining district and those sampled within the district. The Kruskal-Wallis test is a non-parametric test, which therefore does not assume a normal distribution of data, based on medians, and used to compare different populations of small sizes (Zolfaghari et al., 2018). This test is then adapted to our preliminary study in the Orbiel valley.

3. Results

3.1 Morpho-genetic description, classification and metal(loid) concentrations of soils

The different soil profiles from the different lithologies are described in Supplementary Information SI-1. According to field observations and the international World Reference Base classification (WRB from FAO, 2015), among all soils studied, 3 belong to Luvisols (*SPd, SPe, SRk*), 3 can be classified as

Leptosols (*SPf, SPh, SPi-j*), 2 of them belong to Cambisols (*SPg, k1*) and the last one can be classified as Calcisol (*k2b*), as shown in SI-1.

Soil metal(oïd) concentrations are reported in Table 1 for 14 elements (As, Cd, Co, Cr, Cu, Fe, Mn, Ni, Pb, Sb, Ti, U, V, Zn). The first Kruskal-Wallis test performed in the soil data revealed that surface horizons and substratum or C horizon did not exhibit difference in terms of elements concentrations. Consequently, data from all horizons were considered for the following presentation of the results. The second Kruskal-Wallis test - comparing uphill soils and soils sampled within the mining district area - showed significant differences for As, Cd, Mn, Pb, Sb, U, V and Zn. For this first group of elements, soils located uphill of the district exhibited lower concentrations, except for U and V (see Table 1). For U, we think the difference of concentration should be related to the lithology behind these two soils [k2 (sandstone) and k2b (dolomitc limestone)]. Sandstone are generally poor in U and carbonates exhibit generally lower U concentration than felsic rocks (Condie, 1993). On the contrary, Cr, Co, Cu, Fe, Ni and Ti did not show significant differences between soils uphill and within the mining district. This latter set of elements will be called group 2. Considering the uphill soils, we classified the elements by decreasing range of concentrations (in $mg.kg^{-1}$ except Fe and Ti in %): Fe (2.29 – 5.09%) > Ti (0.37 – 0.50%) > Mn (200 – 1600) > V (103.6 – 136.5) > Zn (44.8 – 153.5) > Cr (68.5 – 94.4) > As (35.6 – 75.1) > Cu (200 – 70.2) > Pb (27.0 – 61.9) > Ni (11.0 – 43.1) > Co (2.6 – 18.9) > U (2.13 – 2.91) > Sb (0.32 – 6.25) > Cd (0.15 – 0.35). Arsenic concentrations range from 88.1 to 162.6 $mg.kg^{-1}$ within the district, i.e. higher values than uphill of the district (35.6 to 75.1 $mg.kg^{-1}$). A more detailed comparison of As concentrations in soils (location / depth) is given in supplementary information SI-2

3.2 Metal(loid) concentrations in sediments

Metal(loid) concentrations in sediments are reported in Table 2 for all the sampled rivers. Considering the Orbiel River, we classified elements by decreasing order of concentration (in $mg.kg^{-1}$

except Fe and Ti in %): Fe (0.68 – 6.85%) > Ti (0.05 – 0.53%) > Mn (160 – 1050) > Pb (17.3 – 832.5) > As (7.7 – 515) > Zn (66.8 – 204.4) > V (14.6 – 152.7) > Cr (8.4 – 120.1) > Cu (2.6 – 99.0) > Ni (4.2 – 61.1) > Co (2.4 – 21.1) > Sb (0.02 – 5.11) > U (0.64 – 3.51) > Cd (0.1 – 0.98). Arsenic concentrations increase along the watercourse of the Orbiel River, from 8 $mg.kg^{-1}$ upstream, to 515 $mg.kg^{-1}$ downstream (Gué de Lassac sampling point, see Figure 2). We observed that precipitates collected in the excavation of the floodplain bordering the Orbiel River showed very high As (1.44 – 2.79%) and Fe (11.1 – 14.1%) concentrations. In the case of the Grésillou River, it comes the following range of concentrations (in $mg.kg^{-1}$ except Fe and Ti in %) for river sediments: Fe (3.96 – 9.58%) > Ti (0.06 – 0.28%) > As (118 – 6472) > Mn (100 – 980) > Cu (46.0 – 409.2) > Pb (20.1 – 202.3) > Zn (91.2 – 185.1) > V (89.5 – 136.3) > Cr (62.3 – 96.6) > Ni (30.6 – 52.2) > Sb (0.67 – 36.17) > Co (11.5 – 21.1) > U (2.16 – 3.37) > Cd (0.21 – 1.64). In the Grésillou River, the As sediment concentrations, which can reach up to 0.6%, were much higher than in the bed Orbiel River sediments. The sample LAG-1, collected in the schoolyard of Lastours, showed that suspended sediments transported during the flash flood by the Grésillou River can have a very high As content, i.e. 873 $mg.kg^{-1}$. It can also be noted that the sediment Co, Cu and Cd concentrations were in a high range in this river. For the Russec River, the following order was observed (concentrations in $mg.kg^{-1}$ except Fe and Ti in %): Fe (1.86 – 4.85%) > Ti (0.09 – 0.26%) Mn (290 – 970) > As (143 – 631) > V (45.5 – 127.2) > Cu (26.1 – 107.4) > Cr (30.4 – 83.1) > Pb (28.1 – 54.1) > Ni (15.9- 50.0) > Co (6.7 – 21.0) > U (1.17 – 3.74) > Sb (1.44 – 3.43) > Cd (0.23-0.70). We observed that ANG-1 and ANG-3 samples present a similar high As concentration with 554 and 631 $mg.kg^{-1}$, respectively. As a reminder, these two samples were collected at the same location (as mud in the field) at two different times (November, 2018, and January, 2019). ANG-2 and ANG-4 present an As concentration of 470 and 143 $mg.kg^{-1}$, respectively.

Globally, As appears to be one of the analysed elements present with the highest concentrations for the three monitored rivers. On the other hand, samples ANG-1 to ANG-3, collected at the wine castle

Saint-Angel and deposited after the flash flood of October 14-15, 2018, showed very high concentrations of As, Cu, Cr and Mn compared to other sediments collected in the Russec River bed.

4. Discussion

4.1 Determination of the pedo-geochemical background (PGB) of the Salsigne mining district

Equation (3) was used to calculate the PGB for a given element, as proposed by Reimann et al. (2005).

$$PGB = Median \pm 2 \times MAD \quad \text{(Eq. 3)}$$

where *MAD* corresponds to the median absolute deviation. It has been proven to be less sensitive to extreme values than the "classical" equation (mean ± 2 × standard deviation), and therefore is now being used in several studies focused on the definition of a geochemical background (e.g. Esmaeili et al., 2014; Tapia et al., 2012; Rothwell and Cooke, 2015). Depending on groups 1 or 2, the median and the MAD were calculated on either all soil samples, i.e. soils located uphill and soils located within the mining district, or only on soils located uphill of the district. Thus, for group 1 elements, the PGB was only based on soils located uphill of the district. On the contrary, for group 2 elements, the PGB was based on all soil samples. Median and MAD values were calculated considering all sub-samples from each soil, *i.e.* each depth. Globally, the total numbers of samples for the calculations were 19 for group 1 and 23 for group 2. This method ensured that the calculated PGB included both the geological variability and the variability vs. depth due to pedogenesis. The set of estimated PGB values, considering the 14 selected elements for the Orbiel valley soils, was reported in Table 3. For As, the PGB for the Orbiel valley is estimated to 44 ± 12 $mg.kg^{-1}$. It can be observed that the PGB ranges of Co, Ni, Pb, Sb and Zn were quite wide: 13 ± 10, 28 ± 18, 38 ± 21, 0.9 ± 1.2 and 92 ± 44 $mg.kg^{-1}$, respectively. These broad ranges of Co, Ni, Pb, Sb and Zn concentrations could be due to the natural heterogeneity among the soils in the area.

The PGB determined in the Orbiel valley are then compared to median values (baselines) obtained for soils at the scale of France (Saby et al., 2019a,b) and Europe (Salimen et al., 2005), in the framework of the RMQS (https://www.gissol.fr/) and FOREGS (http://weppi.gtk.fi/publ/foregsatlas/) programs, respectively (Table 3). It comes that these two baselines appear to be very similar, and significantly lower than the PGB calculated in this Orbiel area. Estimated median concentrations, or PGB in the case of Orbiel soils, for As, Cd, Cr, Cu, Pb, V and Zn, seem to be significantly higher in soils from the Orbiel valley than median concentrations observed in soils at the French or European scales. As and other trace metal and metalloid contents in soils and sediments in the vicinity of Au mining areas and As-rich deposits are known to be higher than those found in area with lower mineral indexes, so much so that arsenic has long been used as a geochemical indicator of the presence of mining potential by geologists. The values we find for the geochemical background of the soils of the Orbiel Valley for As, Cu, Pb and Zn (As: 44 ± 12 mg.kg^{-1}; Cu: 38 ± 16; Pb: 38 ± 21, and Zn: 92 ± 44) are comparable to those of other mining provinces in the published literature. Threshold concentration in As, Cu, Pb and Zn for natural geochemical background in soils in the surroundings of mines located in the Iberian Pyrite Belt in the South of Portugal (Pelica et al., 2018 and references therein) are respectively 50, 300, 55 and 140 mg.kg^{-1} for the Neves-Corvo mine area (copper-rich deposits) and 50, 260, 30-90 and 150-250 mg.kg^{-1} for the Aljustrel mine area (lead-zinc rich deposits). In the Oruro mining region of Bolivia (Andean tin belt), the work of Tapia et al. (2012) determined the geochemical background (in the form [minimum; median; maximum]) for As at [38; 52; 72] mg.kg^{-1}, for Cu with [40; 52; 66] mg.kg^{-1} and Zn with [104; 119; 147] mg.kg^{-1}. The natural richness in As in soils located in mining environments is not always verified. Indeed, there are mining environments with low arsenic geochemical background values such as in the vicinity of the Cachoeira Au deposit in the Para state in Brazil where the deep ferralitic soils display geochemical background in As very low, with a mean concentration varying between 0.7 to 6 mg.kg^{-1}, comparable to values for tropical forested

soils without any anthropic influence (Souza Neto et al., 2020). Soils from the old mining area of the Antiform of Martinamor in Spain display As median concentrations of 26 $mg.kg^{-1}$ (García-Sánchez et al., 2010). In Poland, Galuszka et al. (2018) investigated soils geochemistry in the vicinity of an historic lead mining area (Mt. Karczowka) and found concentration values for geochemical background for As of respectively 8-16 $mg.kg^{-1}$. Similar geochemical background values were determined from the sediment study for the state of Morelos, Mexico with 12.5 $mg.kg^{-1}$ As (Barats et al., 2020). On the opposite, other studies have shown higher values for the geochemical background of As, in particular, a British Geological Survey study for a former As mine in Devon, England, determined a geochemical background in soils of 93 $mg.kg^{-1}$ (Palumbo-Roe and Klinck, 2007). The recently published geochemical background data of the Orbiel valley by Melleton and Girardeau (2019) have obtained " PGB ranges between 45 and 339 $mg.kg^{-1}$ for As, depending on the geological formation. Unfortunately, this PGB cannot be used in the present study since it was defined using data previously selected and chosen for another use, i.e. to calculate mineralization indices from the "national mining inventory" (Lambert, 2005). Moreover, data to establish these so-called PGBs have been lacking from the point of view of sampling information (e.g., sampling date, depth, sampling protocol), analytical techniques (limits of detection/quantification) or the mathematical relationship used. Compared to our study, for which As PGB was estimated to 44 ± 12 $mg.kg^{-1}$, it is obvious that such a difference would have strong impacts on the establishment of an objective diagnostic of the contamination by As. In conclusion, the establishment of the geochemical background, which can vary greatly depending on local lithology and pedogenetic processes, needs to be considered with particular attention on a case by case basis. Using geochemical background data~~,~~ which did not follow the PGB determination guidelines, could be considered as a wrong way leading on the one hand to overestimate PGB data and on the other hand to under-estimate the impact of human activities in relation to mining on the global environment contamination of the Orbiel valley.

405

4.2 Enrichment factor in Salsigne ‘soils compared to soil national and international references

We calculated the EF of the soils of the Orbiel valley (PGB values) with respect to the baselines obtained for the soils at the scale of France (Saby et al., 2019a,b) and Europe (Salimen et al., 2005) (see paragraph 4.1), and with respect to upper crust data from Taylor and McLennan (1985) and Rudnick and Gao (2003) (Figure 3). Exception of As and Sb, all the references used give more or less the same flat pattern of enrichment factors, suggesting that our values of PGB were very similar to both chemical composition of the upper crust and soil baselines (France, Europe). The As EF estimated in our work is 8 times higher than the European soil baseline and upper crust data from Rudnick and Gao (2003), and very high, around 30 times more, with respect to the upper crust data from Taylor and McLennan (1985). We also observed that our As PGB value is close to the value proposed by Saby et al. (2019a,b) for the baseline of soils from French territory. In the case of Sb, the EF value is around 7 times higher than the upper crust one (Taylor and McLennan, 1985). Our data set suggests a relative natural As enrichment for the preserved soils within the Orbiel valley. Finally, the data homogeneity with respect to the different references underlines the data robustness and the choice to use them as a local reference for studying sediments of the Orbiel valley (see paragraph 4.3).

4.3 Contamination of sediments by metal(loid)s

For sediment metal(loid)s of the Orbiel valley rivers (Orbiel and its tributaries Russec and Grésillou), EF values were calculated from normalization with respect to Ti as before and (Eq. 1) by using Y = sediment data and Z = PGB data (see Figure 4). From left to right one goes from upstream to downstream for each river. Samples deposited both by the Grésillou River in the Lastours schoolyard and by the Russec River in the Saint-Angel wine castle during this event are reported in Figure 4, in order to better assess the potential risks involved for human health after flash flood of October 14-15, 2018. It should be noted that for the Russec River, all samples were collected in its downstream part,

just before the confluence with the Orbiel River (see Figure 2). Therefore, we cannot compare sediment chemical composition before and after former mine extraction/storage areas for the Russec River.

For the Grésillou River (NAU, NAD and LAG sites, Figure 4), we found that As, Pb, Sb, Cd, Co, Cu and Fe have high EF values (2.3 < EF < 1042), while Mn, Ni, Cr, U, V and Zn exhibit low to moderate EF values (1.5 < EF < 10.0). Given the limited number of samples, it is thus difficult to determine the difference in concentrations between upstream (NAU) and downstream (NAD) points compared to the Nartau storage area. However, it clearly appears that the EF values of Grésillou sediments were higher after the Nartau deposit area than upstream (NAU). By considering the LAG-1 sample, we can introduce constraints on the chemical composition of suspended sediments transported by the Grésillou River during the flash flood on October 14-15, 2018. In that specific case, it comes that the sediment EFs were 190, 108, 33, 20 and 13 for As, Sb, Cd, Pb and Cu, respectively. For all these elements the EF was particularly high. We have reported on the Supplementary Information (SI-4) the granulometry of some of the sediment samples presented in this study. We observed that the suspended sediments from the flood of October, 2018, such as LAG-1 have the finest particle size. The high EF observed are not surprising because the finest fraction is generally more concentrated than the coarser one; this finest fraction may contain clays and Fe oxyhydroxydes, minerals known to control metals and metalloids.

For the Russec River (Figure 4), we can classify analyzed elements into three groups: (i) As, Cd, Cu, and Sb with high enrichment compared to the geochemical background, 1.5 < EF < 27.5, the highest EF values being for As (9 – 27.5); (ii) Pb with moderate EF values, 1.8 < EF < 6.8; and (iii) Co, Zn, Fe, Mn, U, Ni, Cr, and V with low EF values or no enrichment, 0.9 < EF < 3.3. Although we did not have sediments from the upstream part of this river, we can nevertheless observe that the sediments from the downstream part are strongly impacted by anthropogenic activities and most likely the former mines or mine waste storage areas located in the Russec River watershed with respect to As, Cd, Sb and Cu. It is

important to notify that the suspended sediments deposited in the confluence area between Orbiel and Russec rivers (ANG-1 and ANG-3), after the flood of October, 2018, are marked by high EF for these elements (As, Cd, Sb, and Cu) since these EFs are between 5 (Cu) and 20 (As). Again, like for the suspended sediment from the Gresillou River, suspended sediment from the Russec river exhibit a finer granulometry which can explain the high EFs of these specific samples.

For the Orbiel River, we found that some elements show a regular increase in the EF values from upstream to downstream. This is the case for As, Cr, Cu, Fe, Ni, Sb and V, which have EF values close to 1, i.e. no enrichment, in the upstream part, and which can reach 74, 4.1, 6, 4.5, 4.8, 11 and 3.5, respectively, downstream at the Gué de Lassac location (GUE). This statement revealed a strong progressive enrichment of sediments in these elements relative to the PGB going downstream. The Orbiel River, flowing from north to south, crosses the old mining zone (former mines and current storage zones) and its sediments were gradually enriched in As, Cr, Cu, Fe, Ni, Sb and V. The EF values decreased at the Water Treatment Station (WTS) and then increased again between WTS and the Gué de Lassac sites. In the case of Co, Mn and Zn, the EF values were low, close to 2, and constant along the river. However, there were two peculiarities: (i) the EF values were high for Zn and Pb at Miraval-Cabardès, the most upstream point of the Orbiel River; and (ii) the systematic increased in Mn and Co EF values between Lastours (LAS) and Pont de Limousis (LIM), at Moulin d'Artigues (ART) sites. For Pb and U, the EF values were constant and low, up to the GUE site, where a significant increase occurred. For Cd, high EF values, around 5, were calculated, more or less constant from upstream to downstream, with an increase at the GUE site. If we return specifically to the case of As, the EF calculated for the Orbiel and Russec rivers sediments (up to 100) appear to be in the high range of values reported in the literature while the EF calculated for the Gresillou River sediments (up to 1000) are much higher ($1 < EF < 285$, Au Giant Mine in Yellowknife, USA, Cheney et al., 2020; $1 < EF < 133$, Oruro mine, Bolivia, Tapia et al., 2012).

The sediment contamination, i.e. excess of element with respect to geochemical background, could be explained by the two following ways: either by transportation of primary bearing minerals (for example sulphides) or secondary minerals such as iron arsenates (scorodite), characterized at the Nartau site (Lucia Perez Serrano, pers. com.), which were extracted by mechanical weathering and carried from upstream to downstream; or by a chemical transfer from the dissolved phase (e.g., < 0.20 µm) to the particulate phase (e.g., > 0.20 µm) via sorption process (Sigg et al., 2014). We know that the dissolved As charge of the Orbiel River water is also increasing from upstream to downstream (Khaska et al., 2015) by the input of water rich in As, during stable hydrological periods or during extreme events (flash floods as in October, 2018) relatively frequent in this region of Southern France (Raynaud et al., 2015). By studying As concentrations and $^{87}Sr/^{86}Sr$ ratio in surface and ground water, Khaska et al. (2015) have showed that most of the As transported by the Orbiel River originate from leaching of Ca-arsenate stored on site. These Ca-arsenate were produced by the WTS to remove As from contaminated waters, As being co-precipitated with whitewash as $Ca_3(AsO_4)_2$.

Numerous studies have shown the major role of Fe minerals (particularly hydrous iron oxides or iron sulfate minerals), which control the arsenic fate in the environments impacted by mining activity (e.g., Casiot et al., 2003; Sanchez-Espana et al., 2005). In this study, the Fe-As relationship (see Supplementary Information SI-3) also suggested a control of arsenic by Fe minerals in the Orbiel valley sediments, at least for the most concentrated samples. As mentioned before, a preliminary study conducted on the waste storage area of Nartau identified the presence of scorodite, a hydrated iron arsenate ($FeAsO_4 \cdot 2H_2O$) in abundant quantities. As this area is absolutely not isolated, these wastes can be mobilized towards the Gresillou and the Orbiel rivers.

The calculation of the geoaccumulation index (Müller, 1969) is another method for assessing the degree of metal and metalloids contamination of sediments in the Orbiel Valley. According to this index (see section 2.5), some samples may be extremely contaminated with respect to Cr (Water Treatment Station, WTS), Pb (WTS) and Sb (downstream Grésillou). Others sediments are strongly to extremely

contaminated with respect to As (WTS, Gué de Lassac, suspended sediments from the Grésillou and Orbiel/Russec), Cd (Gue de Lassac), Cr (WTS), Cu (downstream Gresillou), Pb (WTS) and Sb (downstream Gresillou). Considering this index, it appears that most of the sediments from the Orbiel River and its two tributaries, Russec and Gresillou, are moderately to extremely contaminated in As. Finally, this index gives results consistent with those of the enrichment factors.

From our set of data, it was possible to compare the measured As concentrations in the sediments of the Orbiel Valley with those from other environments, such as rivers, deltas, lakes, in preserved area [1-14] or on the contrary, in strongly impacted by human activities due to mining or mineral processing [15-22] (Figure 5). This comparison, which is not exhaustive, can nevertheless give us some lessons:

i) In the case of preserved environments, As concentrations range from a few $mg.kg^{-1}$ to a few dozen $mg.kg^{-1}$ (typically < 50 $mg.kg^{-1}$). Moreover, estimates of As average suspended sediment concentrations for major world rivers have been published, yielding 36 (+/- 27) $mg.kg^{-1}$ (Viers et al., 2009), 5 $mg.kg^{-1}$ (Martin and Meybeck, 1976) or 14 $mg.kg^{-1}$ (Savenko, 2006).

ii) Impacted sediment concentrations can reach several thousands of $mg.kg^{-1}$.

iii) Finally, this figure shows that sediment concentrations collected in the Orbiel valley, after the Salsigne mining district area, can reach the highest values measured elsewhere in strongly impacted zones.

5. Conclusion

This first study conducted on the soils and sediments of the Orbiel valley enabled us to obtain a few important results:

i) we first determined pedo-geochemical background (PGB) concentrations for As and also other metal(loid) elements. It appears that compared to soil baselines at national or European level, pristine soils of the Orbiel valley present a marked natural enrichment for As and Sb, with concentrations of 44 ± 12 mg.kg^{-1} and 0.9 ± 1.2 mg.kg^{-1}, respectively. The other elements belong to the magnitude order of soil baselines at national or European level.

ii) The PGB was then used as a local reference to assess the level of contamination of sediments collected along the Orbiel River and two of its major tributaries. We showed the contamination of riverine sediments by past mining activity and/or current storage areas of the former mining district of Salsigne. Indeed, if some peculiarities may appear from one river to another, it appears that the sediments of these rivers are strongly impacted for As, Cu, Sb and Pb after the district mining area. At Gué de Lassac station, at the outlet of the mining district, the enrichment factors can reach 74, 15, 11 and 6 for As, Pb, Sb and Cu, respectively.

iii) Finally, by collecting sediments that have been transported during and deposited after the flash flood of October 14-15, 2018, we can estimate the chemical composition of the suspended sediments transported by the rivers of the valley. In particular, the concentrations of As in suspended samples from the Grésillou River have reached 870 mg.kg^{-1}. In the case of the Russec and Orbiel rivers, suspended sediment concentrations belong to the range 143 – 631 mg.kg^{-1}.

Finally, following these new insights brought by this preliminary study, further studies are currently in progress in the Orbiel valley, based on a multidisciplinary approach in order to better take into account the different environmental compartments and to better understand elemental transfers occurring between water, soil, vegetation and atmosphere. The major issue will concern the population health by proposing adapted mitigation solutions in a context of social and political tensions facing the environmental and health challenges of this Orbiel valley.

Acknowledgements

This work was supported by the EC2CO program of the INSU/CNRS. We express our gratitude to José Darrozes for its help during the field trips, Rémi Freydier and Mylène Marie (HSM laboratory, Montpellier), Léa Causse (AETE-ISO platform, Montpellier) for their assistance in analyses. We would like to thank the staff of the management department of the LCA and GET laboratories, without which nothing could have be achieved.

References

Barats, A., Renac, C., Orani, A.M., Durrieu, G., Saint Martin, H., Esteller, M.V., Garrido Hoyos, S.E., 2020. Tracing source and mobility of arsenic and trace elements in a hydrosystem impacted by past mining activities (Morelos state, Mexico). Sci. Total Environ. 712, 135565.

Berger, G.M., Boyer, F., Debat, P., Demange, M., Freytet, P., Marchal, J.P., Mazéas, H., Vautrelle, C., 1993. Notice explicative, Carte géol. France (1/50 000), feuille Carcassonne (1037) ». Orléans, BRGM.

Borba, R.P., Figueiredo, B.R., Rawlins, B., Matschullat, J., 2003. Geochemical distribution of arsenic in waters, sediments and weathered gold mineralized rocks from Iron Quadrangle, Brazil. Environ. Geol. 44, 39–52. DOI:10.1007/s00254-002-0733-6

Bouchot, V., Ledru, P., Lerouge, C., Lescuyer, J-L., 2005. Late Variscan mineralizing systems related to orogenic processes: The French Massif Central. Ore Geol. Rev. 27, 169-197. DOI:10.1016/j.oregeorev.2005.07.017

Bulka, C.M., Jones, R.M., Turyk, M.E., Stayner, L.T., Argos, M., 2016. Arsenic in drinking water and prostate cancer in Illinois counties: An ecologic study. Environ Res. 148, 450-456. https://doi.org/10.1016/j.envres.2016.04.030

Casiot, C., Morin, G., Juillot, F., Bruneel, O., Personné, J-C., Leblanc, M., Duquesne, K., Bonnefoy, V., Elbaz-Poulichet, F., 2003. Bacterial immobilization and oxidation of arsenic in acid mine drainage (Carnoulès creek, France). Water Res. 37, 2929-2936. https://doi.org/10.1016/S0043-1354(03)00080-0

Cassard, D., Feybesse, J.L., Lescuyer, J.L., 1993. Variscan crustal thickening, extension and late overstacking during the Namurian-Westphalian in the Western Montagne Noire (France). Tectonophysics, 222, 33-53.

Chapagain, S.K., Shrestha, S., Du Laing, G., Verloo, M., Kazama, F., 2009. Spatial distribution of arsenic in the intertidal sediments of River Scheldt, Belgium. Environ. Int. 35 (2009) 461–465 https://doi.org/10.1016/j.envint.2008.07.019

Cheney, C. L., Eccles, K. M., Kimpe, L. E., Thienpont, J. R., Korosi, J. B., & Blais, J. M. (2020). Determining the effects of past gold mining using a sediment palaeotoxicity model. Sci. Total Environ., 718, 137308.

Condie, K.C. (1993) Chemical Composition and Evolution of the Upper Continental Crust; Contrasting Results from Surface Samples and Shales. Chem. Geol. 104, 1-37. https://doi.org/10.1016/0009-2541(93)90140-E

Coynel, A., Schafer, J., Blanc, G., Bossy, C., 2007. Scenario of particulate trace metal and metalloid transport during a major flood event inferred from transient geochemical signals. Appl. Geochem. 22, 821–836. https://doi.org/10.1016/j.seares.2016.08.005

Coynel, A., Gorse, G.,Curti, C., Schafer, J., Grosbois C., Morelli G., Ducassou, E., Blanc G., Maillet, G.M., Mojtahid, M., 2016. Spatial distribution of trace elements in the surface sediments of a

majorEuropean estuary (Loire Estuary, France): Source identification andevaluation of anthropogenic contribution. J. Sea Res. 118, 77-91. https://doi.org/10.1016/j.seares.2016.08.005

Datta, D.K., Subramanian, V., 1997. Texture and mineralogy of sediments from the Ganges-Brahmaputra-Meghna river system in the Bengal basin, Bangladesh and their environmental implications. Environ. Geol. 30, 181–188. DOI:10.1007/s002540050145

Debat, P., Mouline, M.-P., Féraud, J., Cosson, J., 1971. Carte géologique de la France à 1/50000 : Mazamet.

Demange, M., Pascal, M.-L., Raimbault, L., Armand, J., Forette, M.C., Serment, R., Touil, A., 2006. The Salsigne Au-As-Bi-Ag-Cu Deposit, France. Economic Geology 101/1, 199-234. https://doi.org/10.2113/gsecongeo.101.1.199.

Desaulty, A.-M., Negrel, P., Kloppmann, W., 2016. Diagnostic multi-isotopique sur le site de La Combe du Saut (district de Salsigne - Aude). Rapport final. BRGM/RP-65493-FR, 69 p.

Duker, A.A., Carranza, E.J.M., Hale, M., 2005. Arsenic geochemistry and health. Environ. Int. 31/5, 631-41. https://doi.org/10.1016/j.envint.2004.10.020.

Esmaeili, A., Moore, F., Keshavarzi, B., Jaafarzadeh, N., Kermani, M., 2014. A geochemical survey of heavy metals in agricultural and background soils of the Isfahan industrial zone, Iran. Catena 121, 88-98. https://doi.org/10.1016/j.catena.2014.05.003.

Espinoza, E., Armienta, M.A., Cruz, O., Aguayo, A., Ceniceros, N., 2009. Geochemical distribution of arsenic, cadmium, lead and zinc in river sediments affected by tailings in Zimapán, a historical polymetalic mining zone of México. Environ. Geol. 58, 1467-1477. http://dx.doi.org/10.1007/s00254-008-1649-6

Even, E., Masuda H., Shibata, T., Nojima, A., Sakamoto, Y., Murasaki, Y., Chiba, H., 2017. Geochemical distribution and fate of arsenic in water and sediments of rivers from the Hokusetsu area, Japan. J. Hydrol: Reg Stud. 9, 34-47. https://doi.org/10.1016/j.ejrh.2016.09.008

Fabre, J.-M., Domergue, C., Dabosi, F., 2016. Le fer romain de la Montagne Noire. Martys 2 : les débuts. 25 années de recherches pluridisciplinaires (1988-2013). (Supplément à Revue Archéologique de Narbonnaise, 43). Presses universitaires de la Méditerranée, 2016. https://hal.archives-ouvertes.fr/hal-01961822.

Fernandez-Turiel, J.L, Lopez-Soler, A, Llorens, J.F, Querol, X., Acenolaza, P., Durand, F., Lopez, J-P., Medina, M.E., Rossi, J.N., Toselli, A.J., Saavedra, J., 1995. Environmental monitoring using surface water, river sediments, and vegetation: a case study in the Famatina range, La Rioja, NW Argentina. Environ. Int. 21, 807–820. https://doi.org/10.1016/0160-4120(95)00094-8

Gałuszka, A., Migaszewski, Z. M., Dołęgowska, S., Michalik, A., & Duczmal-Czernikiewicz, A., 2015. Geochemical background of potentially toxic trace elements in soils of the historic copper mining area: a case study from Miedzianka Mt., Holy Cross Mountains, south-central Poland. Environ. Earth Sci., 74(6), 4589-4605.

García-Sánchez, A., Alonso-Rojo, P., Santos-Francés, F., 2010. Distribution and mobility of arsenic in sols of a mining area (Western Spain). Sci. Total Environ. 408, 4194-4201.

Géodéris, 2012. Exploitations minières sur le secteur de Salsigne. Concessions de Malabau, Pujol, Lastours, La Caunette, Salsigne, Villanière, Villardonnel. Évaluation et cartographie des aléas mouvements de terrain. Synthèse. Rapport S 2012/109DE- 12LRO2220."

Ikenaka, Y., Nakayama, S.M.M., Muzandu, K., Choongo, K., Teraoka, H., Mizuno, N., Ishizuka, M., 2020. Heavy metal contamination of soil and sediment in Zambia. Afr. J. Environ. Sci. Technol. 4, 729-739.

Girard, A., 2011. Site de Salsigne (Aude). Gestion et surveillance 2007-2010. RP - 59620. BRGM, 2011.

Girardeau, I., 2019. Evaluation des impacts potentiels de la crue d'octobre 2018 sur la qualité des eaux superficielles et des sédiments du bassin versant de l'Orbiel. Rapport final. BRGM/RP-68777-FR, 67p.

Gordeev, V.V., Rachold, V., Vlasova, I.E., 2004. Geochemical behaviour of major and trace elements in suspended particulate material of the Irtysh river, the main tributary of the Ob river, Siberia. Appl Geochem.19, 593–610. https://doi.org/10.1016/j.apgeochem.2003.08.004

Grosbois, C, Courtin-Nomade, A, Martin, M, Bril, H., 2007. Transportation and evolution of trace element bearing phases in stream sediments of a mining-influenced basin (Upper Isle, France). Appl Geochem. 22, 2362–2374. DOI:10.1016/j.apgeochem.2007.05.006

Han, L., Gao, B., Hao, H., Lu, J., Xu, D., 2019. Arsenic pollution of sediments in China: An assessment by geochemical baseline. Sci. Total Environ. 6451, 1983-1991. https://doi.org/10.1016/j.scitotenv.2018.09.381

Hoang, T.H., Bang, S., Kim, K-W., Nguyen M.H., Dang, D.M., 2010. Arsenic in groundwater and sediment in the Mekong River delta, Vietnam. Environ. Pollut. 158, 2648-2658. DOI: 10.1016/j.envpol.2010.05.001

Horckmans, L., Swennen, R., Deckers, J., Maquil, R., 2004. Local background concentrations of trace elements in soils: a case study in the Grand Duchy of Luxembourg. Catena 59/3, 279-304. https://doi.org/10.1016/j.catena.2004.09.004.

Huntsman-Mapila, P., Mapila, T., Letshwenyo, M., Wolski, P., Hemond, C., 2006. Characterization of arsenic occurrence in the waterand sediments of the Okavango Delta, NW Botswana. Appl. Geochem. 21, 1376-1391. https://doi.org/10.1016/j.apgeochem.2006.05.003

Jolivet, C., Arrouays, D., Boulonne, L., Ratié, C., Saby, N., 2016. Le réseau de mesures de la qualité des sols de France (RMQS). Etat d'avancement et premiers résultats. Étude et Gestion des Sols 13/3, 149-64.

Khaska, M., Le Gal La Salle, C., Sassine, L., Cary, L., Bruguier, O., Verdoux, P., 2018. Arsenic and metallic trace elements cycling in the surface water-groundwater-soil continuum down-gradient from a

reclaimed mine area: isotopic imprints. J. Hydrol. 558, 341-355. https://doi.org/10.1016/j.jhydrol.2018.01.031.

Khaska, M., Le Gal La Salle, C., Verdoux, P., Boutin, R., 2015. Tracking natural and anthropogenic origins of dissolved arsenic during surface and groundwater interaction in a post-closure mining context: Isotopic constraints. J. Contaminant Hydrol. 177-178, 122-35. https://doi.org/10.1016/j.jconhyd.2015.03.008.

Lambert, A., 2005. Les données géochimiques et alluvionnaires de l'inventaire minier du territoire national. Constitution d'une base de données exhaustive. Rapport final. BRGM/RP53546-FR, 116 p.

Landrigan, P.J., Fuller, R., Acosta, N.J.R., Adeyi, O., Arnold, R., Basu, N.N., et al., 2018. The Lancet Commission on pollution and health. Lancet 391, 462-512. https://doi: 10.1016/S0140-6736(17)32345-0.

Lebouc, L., Payrastre, O., Bourgin, F., 2019. Reconstitution des débits de pointe des crues du 15 octobre 2018 dans le bassin de l'Aude. Convention DGPR-Ifsttar 2018 n°2201132931 du 22 Mai 2018 - Action 7 appui au SCHAPI. [Rapport de recherche] Institut Français des Sciences et Technologies des Transports, de l'Aménagement et des Réseaux. 2019, 14 p. ffhal-02110612f

Li, Y., Ji, L., Mi., W., Xie, S., Bi, Y., 2021. Health risks from groundwater arsenic on residents in northern China coal-rich region. Sci. Total Environ. 773, 145003. https://doi.org/10.1016/j.scitotenv.2021.145003

Li., S., Wang, M., Yang, Q., Wang, H., Zhu, J., Zheng, B., Zheng, Y., 2013. Enrichment of arsenic in surface water, stream sediments and soils in Tibet. J Geochem Explor. 135, 104–116. https://doi.org/10.1016/j.gexplo.2012.08.020

Mackey, E. , Johnson, C. , Lindstrom, R. , Long, S. , Marlow, A. , Murphy, K. , Paul, R. , Popelka-Filcoff, R. , Rabb, S. , Sieber, J. , Oflaz, R. , Tomlin, B. , Wood, L. , Yen, J. , Yu, L. , Zeisler, R. , Wilson, S. , Adams, M. , Brown, Z. , Lamothe, P. , Taggart, J. , Jones, C. and Nebelsick, J. (2010), Certification of Three NIST Renewal Soil Standard Reference Materials® for Element Content: SRM 2709a San Joaquin Soil, SRM 2710a Montana Soil I, and SRM 2711a Montana Soil II, Special Publication (NIST SP), National Institute of Standards and Technology, Gaithersburg, MD, [online], https://doi.org/10.6028/NIST.SP.260-172 (Accessed April 28, 2021)

Marcoux, E., Lescuyer, J.-L., 1994. Les minerais sulfo-arséniés aurifères de Salsigne, Aude, France ; évolution paragénétique d'une minéralisation tardi-hercynienne syntectonique en contexte sédimentaire. The Canadian Mineralogist 32/1, 159-177.

Martin, J.M., Meybeck, M., 1979. Elemental mass balance of material carried by major world rivers. Mar. Chem. 7, 173–206. https://doi.org/10.1016/0304-4203(79)90039-2

Melleton J., Girardeau I. (2019) - Fond géochimique dans le secteur des anciennes mines d'or de Salsigne (Aude) : apports des données de l'Inventaire minier. Rapport final. BRGM/RP-68771-FR, 79 p., 42 fig., 29 tabl.

Müller, G. (1969). Index of geoaccumulation in the sediments of the Rhine River. Geojournal, 2, 108–118.

Nriagu, J.O., Pacyna, J.M., 1988. Quantitative assessment of worldwide contamination of air, water and soils by trace metals. Nature 333, 134-39. https://doi.org/10.1038/333134a0.

Oyarzun, R., Lillo, J., Higueras, P., Oyarzun, J., Maturana, H., 2004. Strong arsenic enrichment in sediments from the Elqui watershed, Northern Chile: industrial (gold mining at El Indio–Tambo district) vs. geologic processes. J. Geochem. Explor. 84, 53 – 64. https://doi.org/10.1016/j.gexplo.2004.03.002

Palumbo-Roe, B., Klinck, B., 2007. Bioaccessibility of arsenic in mine waste-contaminated soils: A case study from an abandoned arsenic mine in SW England (UK). J Environ. Sci. Health Part A 42(9):1251-61 DOI:10.1080/10934520701435692

Pelica, J., Barbosa, S., Reboredo, F., Lidon, F., Pessoa, F., Calvão, T., 2018. The paradigm of high concentration of metals of natural or anthropogenic origin in soils – The cas of Neves-Corvo mine area (Southern Portugal). J. Geochem. Explor. 186, 12-23.

Plumlee, G.S., Ziegler, T.L., **2007**. The medical geochemistry of dusts, soils and other earth materials. Treatise on Geochemistry, vol. 9. Editor: Barbara Sherwood Lollar. Executive Editors: Heinrich D. Holland and Karl K. Turekian. pp. 612. ISBN 0-08-043751-6. Elsevier, 2003., p. 263-310

Pujol, H., 2014. Tristes mines. Impacts environnementaux et sanitaires de l'industrie extractive. Les Etudes Hospitalières, Bordeaux.

Purves, D., 1985. Trace-Element Contamination of the Environment. Elsevier, Amsterdam - Oxford - New York - Tokyo.

Raynaud, F., Mathieu-Subias, H., Borrell-Estupina, V., Pistre, S., Seidel, J.-L., Van-Exter, S., Montety, V. de, Hernandez, F., 2015. Influence of karstic system on surface flooding in Mediterranean climate, In: G. Lollino et al. (eds.), Engineering Geology for Society and Territory – vol. 3, Springer Int. Pub. Switzerland, pp. 189-193. DOI: 10.1007/978-3-319-09054-2_38

Reimann, C., Filzmoser, P., Garrett, R.G., 2005. Background and threshold: critical comparison of methods of determination. Sci. Total Environ. 346/1, 1-16. https://doi.org/10.1016/j.scitotenv.2004.11.023.

Resongles, E., Casiot, C., Freydier, R., Dezileau, L., Viers, J., Elbaz-Poulichet, F., 2014. Persisting impact of historical mining activity to metal (Pb, Zn, Cd, Tl, Hg) and metalloid (As, Sb) enrichment in sediments of the Gardon River, southern France. Sci. Total Environ. 481, 509–521. https://doi.org/10.1016/j.scitotenv.2014.02.078

Resongles, E., Casiot, C., Freydier, R., Le Gall, M., Elbaz-Poulichet, F., 2015. Variation of dissolved and particulate metal(loid) (As, Cd, Pb, Sb, Tl, Zn) concentrations under varying discharge during a Mediterranean flood in a former mining watershed, the Gardon River (France). J. Geochem. Explor. 158, 132–142. https://doi.org/10.1016/j.gexplo.2015.07.010

Romero, L., Alonso, H., Campanoa, P., Fanfani, L., Cidu, R., Dadea, C., Keegan, T., Thornton, I., Farago, M., 2003. Arsenic enrichment in waters and sediments of the Rio Loa (Second Region, Chile). Appl. Geochem. 18, 1399–1416. https://doi.org/10.1016/S0883-2927(03)00059-3

Rosso, J., Schenone, N., Carrera, A., Cirelli, A., 2013. Concentration of arsenic in water, sediments and fish species from naturally contaminated rivers. Environ. Geochem. Health 35, 201-214. https://doi.org/10.1007/s10653-012-9476-9

Rothwell, K.A., Cooke, M.P., 2015. A comparison of methods used to calculate normal background concentrations of potentially toxic elements for urban soil. Sci. Total Environ. 532, 625-34. https://doi.org/10.1016/j.scitotenv.2015.06.083.

Rudnick, R.L., Gao, S., 2003. Composition of the Continental Crust. Treatise on Geochemistry vol 3, 1-64.

Saby, N., Bertouy, B., Boulonne, L., Bispo, A., Ratié, C., Jolivet, C., 2009a. Statistiques sommaires issues du RMQS sur les données agronomiques et en éléments traces des sols français de 0 à 50 cm. Portail Data INRAE, V4. https://doi.org/10.15454/BNCXYB/2GBDIV.

Saby, N., Thioulouse, J., Jolivet, C., Ratié, C., Boulonne, L., Bispo, A., Arrouays, D., 2009b. Multivariate analysis of the spatial patterns of 8 trace elements using the French soil monitoring network data. Sci. Total Environ. 407, 5644–5652. DOI : doi:10.1016/j.scitotenv.2009.07.002

Saint-Jacques, N., Brown, P., Nautac, L., Boxall, J., Parkere, L., Dummer, T.J.B., 2018. Estimating the risk of bladder and kidney cancer from exposure to low-levels of arsenic in drinking water, Nova Scotia, Canada. Environ. Int. 110, 95-104. https://doi.org/10.1016/j.envint.2017.10.014

Salimen, R. (chief-editor). Geochemical Atlas of Europe. Part 1 - Background Information, Methodology, and Maps. ISBN 951-690-913-2 (electronic version).

Salomons, W., Förstner, U., 1984. Metals in the hydrocycle. Springer, Berlin.

Sanchez Espana J., Lopez Pamo E., Santofimia Pastor E., Reyes Andrés J., Martin Rubi J-A., 2005. The natural attenuation of two acidic effluents in Tharsis and La Zarza-Perrunal mines (Iberian Pyrite Belt, Huelva, Spain). Environ. Geol. 49, 253-266. https://doi.org/10.1007/s00254-005-0083-2

Savenko VS. 2006. Chemical composition of World River's suspended matter. GEOS 2006 [175pp. in Russian]

Schuh, C.E., Jamieson, H.E., Palmer, M.J., Martin, A.J., Blais, J.M., 2019. Controls governing the spatial distribution of sediment arsenic concentrations and solid-phase speciation in a lake impacted by legacy mining pollution. Sci. Total Environ. 654, 563-575. https://doi.org/10.1016/j.scitotenv.2018.11.065

Sigg, L., Behra, P., Stumm, W., 2014. Chimie des milieux aquatiques. 5th ed., Dunod, Paris.

Souza Neto, H.F., Silveira Peireira, W.V., Dias, Y.N., Souza, E.S., Teixeira, R.A., Lima, M.W., Ramos, S.J., Bastos do Amarante, C., Fernandez, A.R., 2020. Environmental and human health risk of arsenic in gold miing areas in the eastern Amazon. Environ. Pollut. 265, 114969.

Tapia, J., Audry, S., Townley, B., Duprey, J.-L., 2012. Geochemical background, baseline and origin of contaminants from sediments in the mining-impacted Altiplano and eastern Cordillera of Oruro, Bolivia. Geochem Explor Environ Anal 12/1, 3-20. https://doi.org/10.1144/1467-7873/10-RA-049.

Taylor, S.R., McLennan, S.M., 1985. The Continental Crust: Its Composition and Evolution. Blackwell, Oxford.

Tollon, F., 1970. Le district aurifère de Salsigne-Aude. Thèse d'Etat, Université Paul Sabatier, Toulouse.

Viers, J., Dupré, B., Gaillardet, J., 2009. Chemical composition of suspended sediments in World Rivers: New insights from a new database. Sci. Total Environ. 407, 853-868. https://doi.org/10.1016/j.scitotenv.2008.09.053

Zolfaghari G, Atash AZS, Sazgar A, 2018. Baseline heavy metals in plant species from some industrial and rural areas: Carcinogenic and non-carcinogenic risk assessment, MethodsX, Volume 5, 43-60. https://doi.org/10.1016/j.mex.2018.01.003.

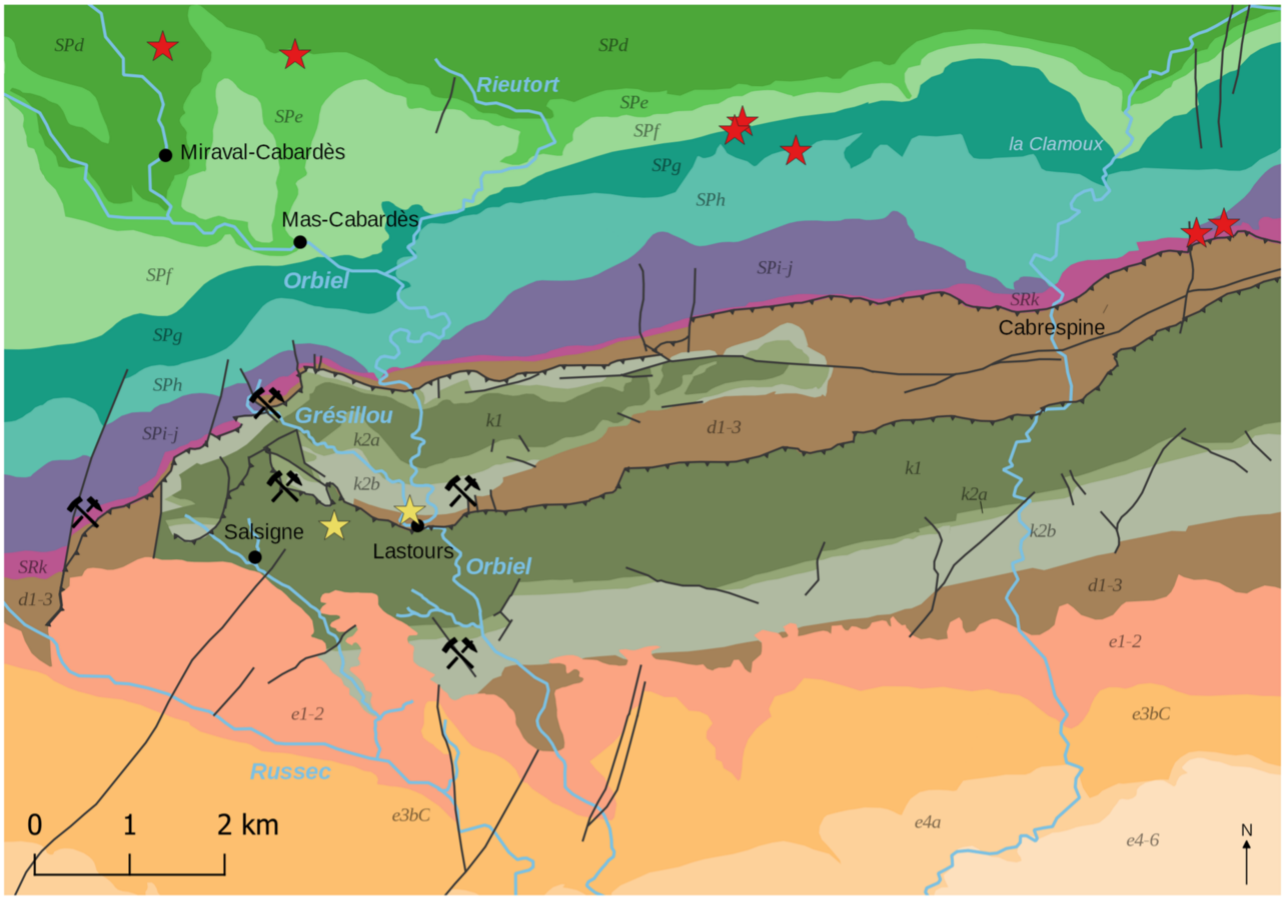

Legend

Cenozoïc

Aquitain Basin

- e4-6 - Carcassonne molasse (upper Ypresian - Bartonian)
- e4-a - Ventenac lacustrine limestones (upper Ypresian)
- e3bC - Alveolinids-bearing limestones (lower Ypresian)
- e1-2 - Conglomerates, sand, silt, lacustrine limestones (Paleocene)

Environment, Structure and Sampling

- Streams
- Faults
- Thrust faults
- Dissused mines
- Soils sampled (geochemical background)
- Soils sampled (for comparison)

Paleozoïc

Minervois nappe

- d1-3 - Indian bead limestones, black limestones, gray dolomites, white limestones, flinty limestones (lower Devonian)
- k2b - Archaeocyathids-bearing dolomitic limestones (lower Cambrian)
- k2a - Alternating sandstones and archaeocyathids- and trilobites-bearing limestones (lower Cambrian)
- k1 - Marcory sandstones (lower Cambrian)

Axial zone

Roc-Suzadou group

- SRk - Conglomerates, sandstones, quartzites (upper Ordovician - Silurian)

Saint-Pons - Cabardès group

- SPi-j - Black schists (Cambrian - Ordovician)
- SPh - Clastic sandstones (Cambrian - Ordovician)
- SPg - Black schists and clastic sandstones, banded schists (Cambrian - Ordovician)
- SPf - Biotite-bearing schists and quartzites (Cambrian - Ordovician)
- SPe - Pelitic sandstones formation of Mas-Cabardès (Cambrian - Ordovician)
- SPd - Metapelitic formation of Miraval-Cabardès (Cambrian - Ordovician)

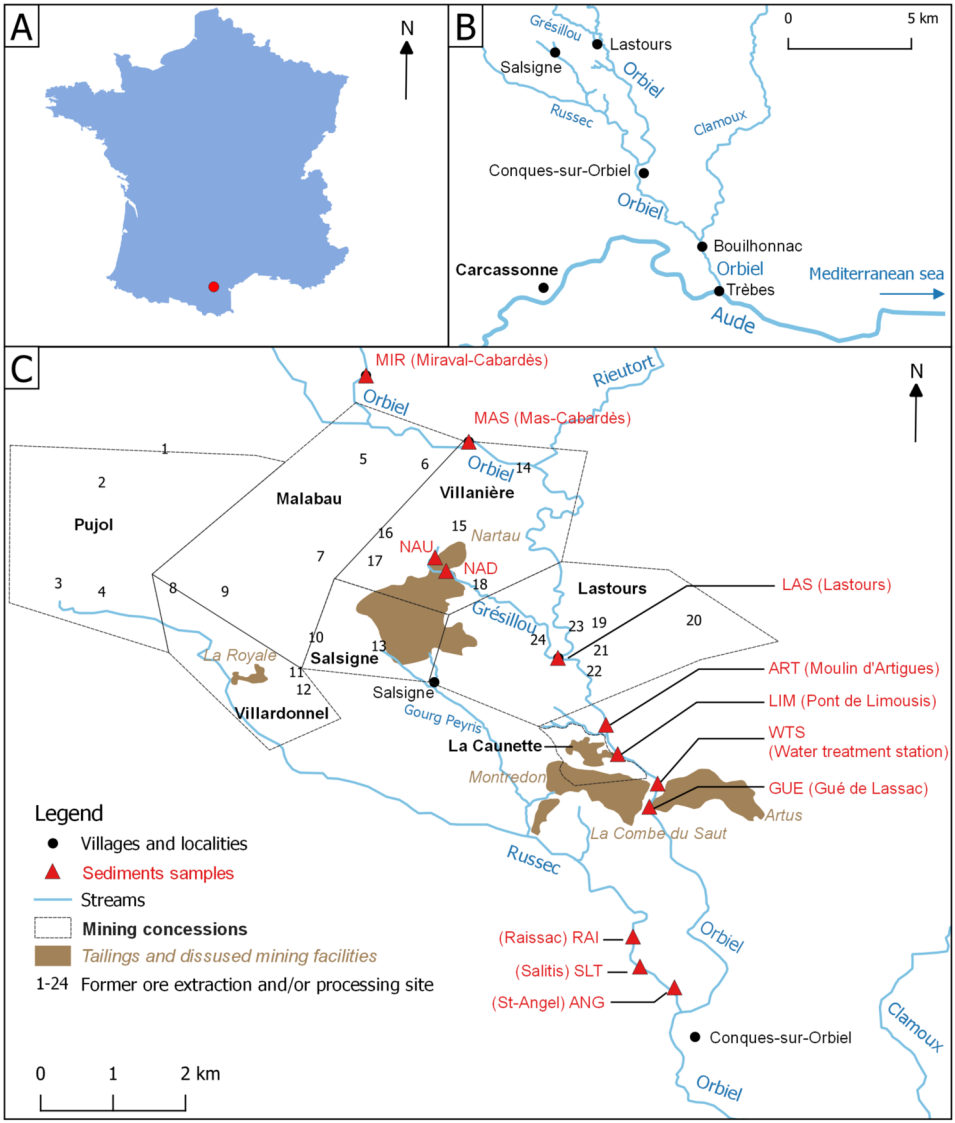
A
N
B
0
5 km
Grésillou
Lastours
Salsigne
Orbiel
Russec
Clamoux
Conques-sur-Orbiel
Orbiel
Bouilhonnac
Carcassonne
Orbiel
Mediterranean sea
Trèbes
Aude
C
N
MIR (Miraval-Cabardès)
Rieutort
Orbiel
MAS (Mas-Cabardès)
Orbiel
Malabau
Villanière
Pujol
Nartau
NAU
NAD
Lastours
LAS (Lastours)
Grésillou
La Royale
Salsigne
Salsigne
Villardonnel
Gourg Peyris
La Caunette
ART (Moulin d'Artigues)
LIM (Pont de Limousis)
WTS
(Water treatment station)
Montredon
GUE (Gué de Lassac)
Artus
La Combe du Saut
Russec
Orbiel
(Raissac) RAI
(Salitis) SLT
(St-Angel) ANG
Conques-sur-Orbiel
Clamoux
Orbiel
Legend
Villages and localities
Sediments samples
Streams
Mining concessions
Tailings and dissused mining facilities
1-24 Former ore extraction and/or processing site
0
1
2 km

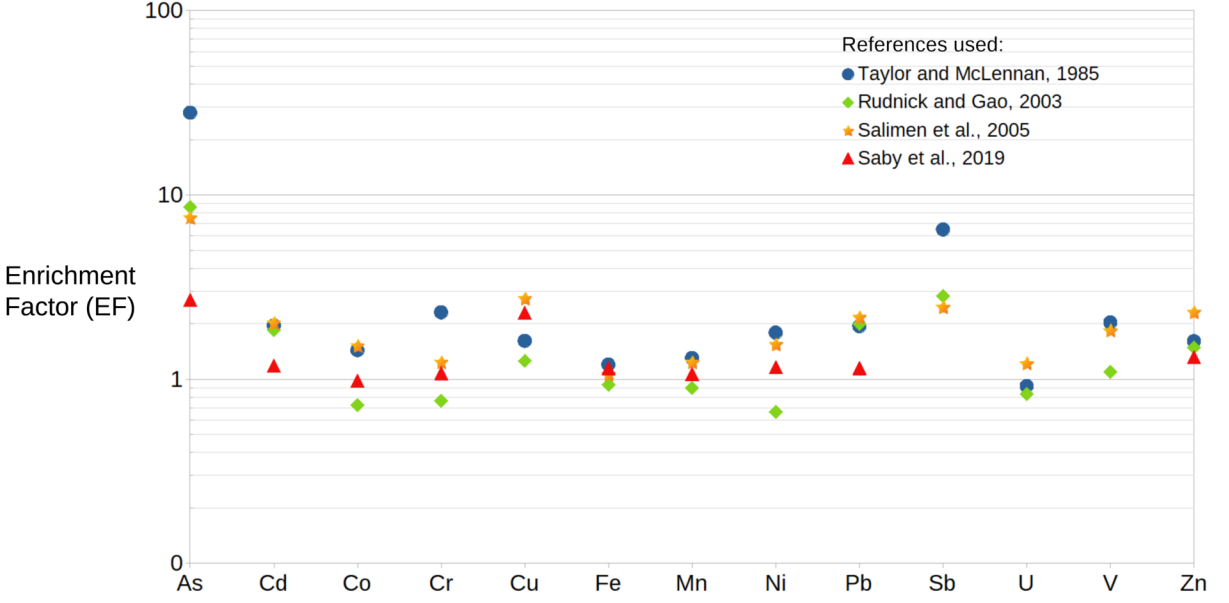
Enrichment Factor (EF)
100
10
1
0
References used:
Taylor and McLennan, 1985
Rudnick and Gao, 2003
Salimen et al., 2005
Saby et al., 2019
As
Cd
Co
Cr
Cu
Fe
Mn
Ni
Pb
Sb
U
V
Zn

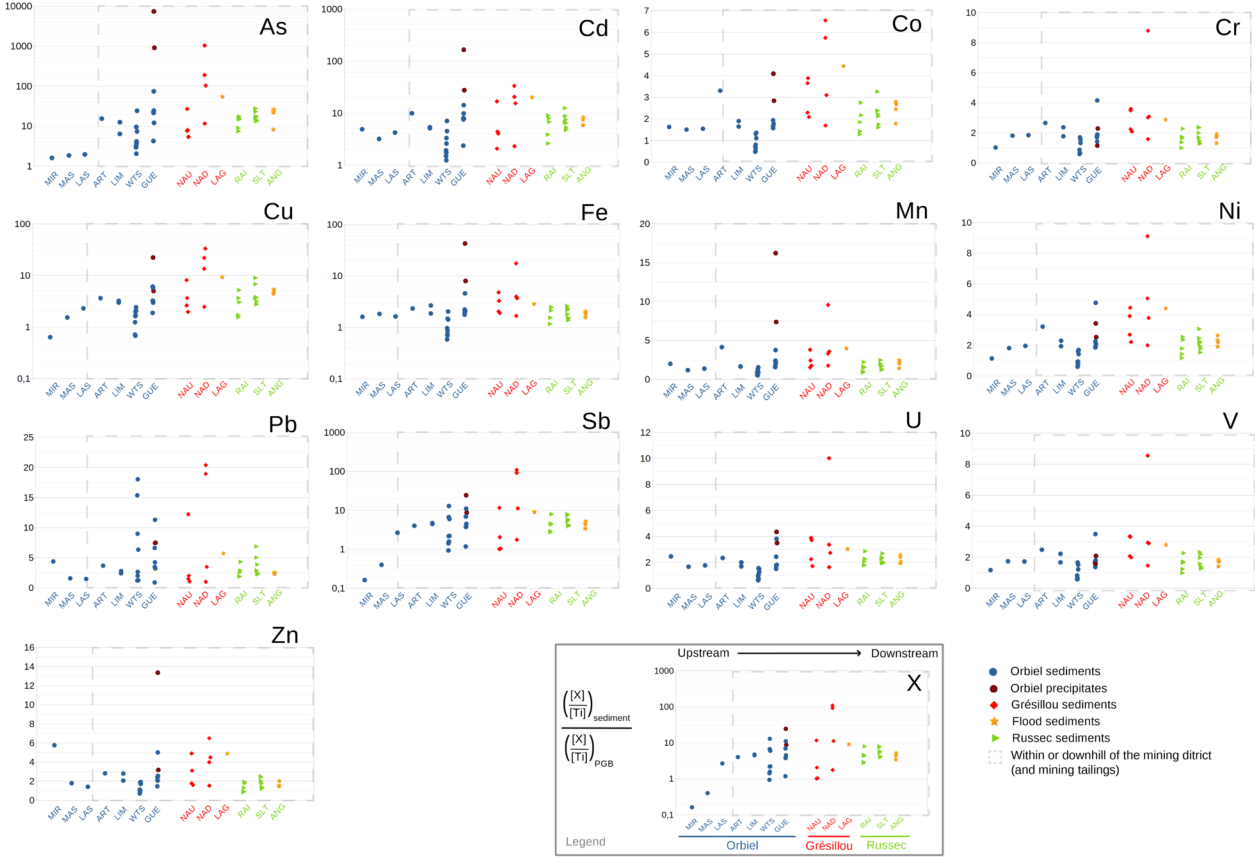
As
Cd
Co
Cr
Cu
Fe
Mn
Ni
Pb
Sb
U
V
Zn
MIR MAS LAS ART LIM WTS GUE NAU NAD LAG RAI SLT ANG
Upstream
Downstream
X
Orbiel
Grésillou
Russec
Legend
Orbiel sediments
Orbiel precipitates
Grésillou sediments
Flood sediments
Russec sediments
Within or downhill of the mining ditrict (and mining tailings)

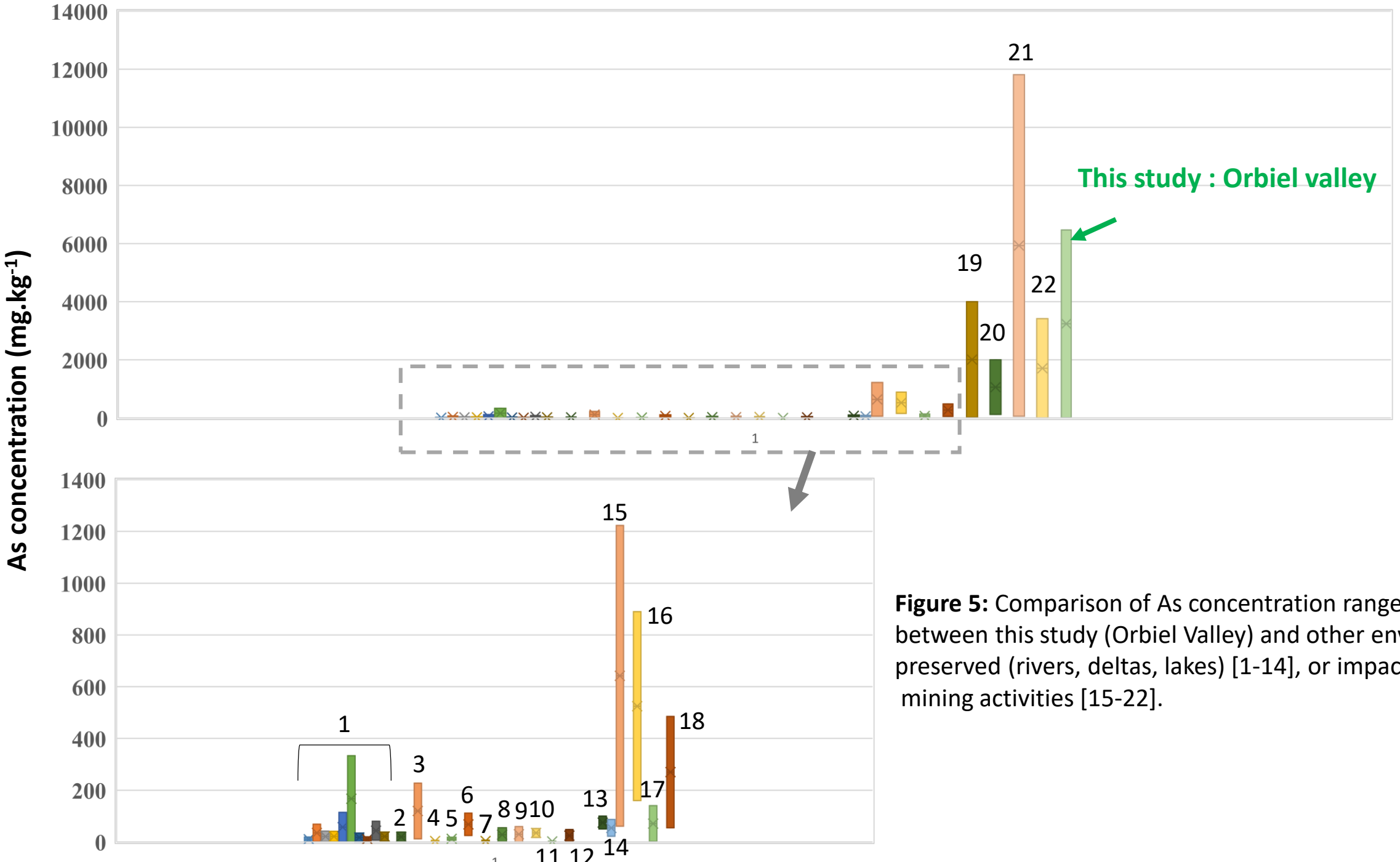

Figure 5: Comparison of As concentration ranges between this study (Orbiel Valley) and other environments: preserved (rivers, deltas, lakes) [1-14], or impacted by mining activities [15-22].

Table 1 : Mean concentrations in metal(oid)s in soils sampled in the Orbiel valley

	Samples	As*	Cd*	Co	Cr	Cu	Fe	Mn*	Ni	Pb*	Sb*	Ti	U*	V*	Zn*
Uphill of the mining district (pedo-geochemical background)	**Spd** (n = 5)	35.6	0.15	12.9	79.6	38.4	3.68	0.07	33.6	27.7	0.32	0.37	2.66	117.3	106.43
	Spe (n = 4)	42.6	0.16	18.9	94.4	48.8	5.09	0.07	43.1	31.1	0.42	0.47	2.72	136.5	153.53
	Spf (n = 2)	47.4	0.30	12.4	77.6	70.2	4.09	0.08	28.2	43.4	1.30	0.41	2.13	117.0	83.75
	Spg (n = 2)	45.0	0.35	5.2	68.5	29.2	3.93	0.03	18.3	61.9	1.64	0.38	2.16	103.6	73.32
	Sph (n = 2)	75.1	0.27	14.1	76.8	23.7	3.69	0.16	27.9	42.6	0.91	0.46	2.18	114.9	90.45
	Spi (n = 2)	47.2	0.18	4.1	89.4	33.2	4.01	0.02	17.0	46.4	6.25	0.50	2.91	131.4	67.68
	Srk (n = 2)	43.0	0.14	2.6	84.2	20.0	2.29	0.02	11.0	31.6	3.68	0.45	2.53	124.3	44.82
Within the mining district	**k1** (n = 2)	88.1	0.31	19.7	82.3	37.1	4.58	0.16	41.6	71.7	4.60	0.50	1.99	114.1	127.21
	k2b (n = 2)	162.6	1.96	8.3	34.8	44.8	2.81	0.16	27.0	162.8	4.60	0.20	1.70	61.2	232.98

Concentrations are given in $mg.kg^{-1}$ except for Fe, Mn and Ti, which are given in %. **n** corresponds to the number of horizons collected for each soil and used for the mean calculation. ***** is displayed when there is a statistical difference (Kruskall-Wallis test, p-value : 0.05) between soils located uphill and within the mining district. For the localisation of the samples refer to Figure 1. Elements are presented in alphabetical order.

Table 2: Concentrations in metal(oid)s in sediments from the Orbiel valley. Concentrations are given in mg.kg-1, or when indicated in % or ‰.

* corresponds to precipitates; ** corresponds to sediments from the October 2018 flood. Elements are presented in alphabetical order.

Stream	Sample	GPS coordinates	Date (mm/yy)	As	Cd	Co	Cr	Cu	Fe %	Mn ‰
Orbiel	MIR-1	43°22'56.1"N 2°20'44.4"E	04/19	7.7 ± *0.2*	0.10 ± *0.00*	2.4 ± *0.1*	8.4 ± *0.2*	2.6 ± *0.1*	0.68 ± *0.02*	0.16 ± *0.00*
	MAS-1	43°22'01.1"N 2°22'22.9"E	04/19	40 ± *1*	0.28 ± *0.01*	9.9 ± *0.2*	66.6 ± *1.7*	28.2 ± *0.7*	3.49 ± *0.09*	0.42 ± *0.01*
	LAS-1	43°20'02.3"N 2°22'41.6"E	04/19	45 ± *1*	0.39 ± *0.01*	10.6 ± *0.3*	71.3 ± *1.8*	44.5 ± *1.1*	3.28 ± *0.08*	0.52 ± *0.01*
	ART-1	43°19'20.5"N 2°23'10.4"E	04/19	225 ± *6*	0.58 ± *0.01*	14.6 ± *0.4*	65.8 ± *1.6*	44.8 ± *1.1*	3.00 ± *0.08*	0.99 ± *0.02*
	LIM-1	43°19'03.4"N 2°23'18.2"E	11/18	234 ± *6*	0.40 ± *0.01*	10.7 ± *0.3*	74.9 ± *1.9*	50.9 ± *1.3*	4.37 ± *0.11*	0.50 ± *0.01*
	LIM-2	43°19'03.4"N 2°23'18.2"E	04/19	134 ± *3*	0.43 ± *0.01*	10.5 ± *0.3*	63.2 ± *1.6*	53.3 ± *1.3*	3.45 ± *0.09*	0.58 ± *0.01*
	WTS-1	43°18'39.0"N 2°23'41.2"E	07/20	136 ± *3*	0.34 ± *0.01*	9.5 ± *0.2*	64.3 ± *1.6*	45.5 ± *1.1*	3.68 ± *0.09*	0.65 ± *0.02*
	WTS-2	43°18'45.7"N 2°23'42.8"E	07/20	83 ± *2*	0.27 ± *0.01*	8.0 ± *0.2*	58.1 ± *1.5*	34.0 ± *0.9*	2.61 ± *0.07*	0.43 ± *0.01*
	WTS-3	43°18'45.7"N 2°23'42.8"E	07/20	165 ± *4*	0.41 ± *0.01*	7.5 ± *0.2*	58.9 ± *1.5*	39.3 ± *1.0*	2.82 ± *0.07*	0.33 ± *0.01*
	WTS-4	43°18'45.7"N 2°23'42.8"E	07/20	93 ± *2*	0.23 ± *0.01*	8.8 ± *0.2*	51.4 ± *1.3*	26.2 ± *0.7*	2.78 ± *0.07*	0.38 ± *0.01*
	WTS-6	43°18'39.0"N 2°23'41.2"E	07/20	169 *4*	0.34 *0.01*	8.4 *0.2*	57.7 *1.4*	34.7 *0.9*	2.94 *0.07*	0.55 *0.01*
	WTS-7	43°18'39.0"N 2°23'41.2"E	07/20	210 *5*	0.59 *0.01*	13.8 *0.3*	63.8 *1.6*	81.9 *2.0*	4.30 *0.11*	1.02 *0.03*
	WTS-8	43°18'39.0"N 2°23'41.2"E	07/20	493 *12*	0.58 *0.01*	8.3 *0.2*	45.7 *1.1*	41.7 *1.0*	3.64 *0.09*	0.52 *0.01*
	WTS-9	43°18'39.0"N 2°23'41.2"E	07/20	417 *10*	0.31 *0.01*	6.8 *0.2*	46.1 *1.2*	60.8 *1.5*	2.88 *0.07*	0.39 *0.01*
	GUE-1	43°18'31.0"N 2°23'37.8"E	11/18	254 ± *6*	0.67 ± *0.02*	11.3 ± *0.3*	67.6 ± *1.7*	53.2 ± *1.3*	3.89 ± *0.10*	0.73 ± *0.02*
	GUE-2 *	43°18'31.0"N 2°23'37.8"E	11/18	27,951 ± *699*	2.50 ± *0.06*	4.6 ± *0.1*	7.4 ± *0.2*	71.0 ± *1.8*	14.05 ± *0.35*	1.00 ± *0.02*
	GUE-3 *	43°18'31.0"N 2°23'37.8"E	12/18	14,408 ± *360*	1.75 ± *0.04*	13.5 ± *0.3*	61.3 ± *1.5*	66.9 ± *1.7*	11.12 ± *0.28*	1.91 ± *0.05*
	GUE-4	43°18'31.0"N 2°23'37.8"E	12/18	436 ± *11*	0.62 ± *0.02*	11.2 ± *0.3*	60.2 ± *1.5*	99.0 ± *2.5*	3.75 ± *0.09*	0.74 ± *0.02*
	GUE-5	43°18'31.0"N 2°23'37.8"E	12/18	121 ± *3*	0.27 ± *0.01*	14.2 ± *0.4*	82.8 ± *2.1*	45.4 ± *1.1*	4.43 ± *0.11*	0.74 ± *0.02*
	GUE-6	43°18'31.0"N 2°23'37.8"E	12/18	415 ± *10*	0.98 ± *0.02*	21.1 ± *0.5*	120.1 ± *3.0*	83.0 ± *2.1*	6.85 ± *0.17*	1.05 ± *0.03*
	GUE-7	43°18'31.0"N 2°23'37.8"E	04/19	1,405 ± *35*	0.75 ± *0.02*	9.8 ± *0.2*	45.7 ± *1.1*	51.4 ± *1.3*	3.38 ± *0.08*	0.75 ± *0.02*
	GUE-8	43°18'31.0"N 2°23'37.8"E	04/19	515 ± *13*	0.73 ± *0.02*	11.4 ± *0.3*	69.8 ± *1.7*	66.1 ± *1.7*	4.15 ± *0.10*	0.70 ± *0.02*
Grésillou	NAU-1	43°21'06.7"N 2°21'26.8"E	12/18	118 ± *3*	0.27 ± *0.01*	17.5 ± *0.4*	90.8 ± *2.3*	46.0 ± *1.2*	4.30 ± *0.11*	0.60 ± *0.01*
	NAU-2	43°21'06.7"N 2°21'26.8"E	12/18	194 ± *5*	0.21 ± *0.01*	17.6 ± *0.4*	96.6 ± *2.4*	56.5 ± *1.4*	4.57 ± *0.11*	0.64 ± *0.02*
	NAU-3	43°21'06.7"N 2°21'26.8"E	12/18	280 ± *7*	0.71 ± *0.02*	11.5 ± *0.3*	61.7 ± *1.5*	71.6 ± *1.8*	4.38 ± *0.11*	0.65 ± *0.02*
	NAU-4	43°21'06.7"N 2°21'26.8"E	04/19	127 ± *3*	0.39 ± *0.01*	14.9 ± *0.4*	83.6 ± *2.1*	39.6 ± *1.0*	3.96 ± *0.10*	0.69 ± *0.02*
	NAD-1	43°20'55.6"N 2°21'31.4"E	11/18	1,509 ± *38*	0.90 ± *0.02*	13.6 ± *0.3*	76.3 ± *1.9*	409.2 ± *10.2*	4.72 ± *0.12*	0.86 ± *0.02*
	NAD-2	43°20'55.6"N 2°21'31.4"E	12/18	352 ± *9*	0.28 ± *0.01*	15.5 ± *0.4*	81.6 ± *2.0*	63.5 ± *1.6*	4.49 ± *0.11*	0.89 ± *0.02*
	NAD-3	43°20'55.6"N 2°21'31.4"E	12/18	6,472 ± *162*	0.51 ± *0.01*	12.3 ± *0.3*	92.7 ± *2.3*	115.4 ± *2.9*	9.58 ± *0.24*	0.98 ± *0.02*
	NAD-4	43°20'55.6"N 2°21'31.4"E	04/19	2,317 ± *58*	1.64 ± *0.04*	21.1 ± *0.5*	62.3 ± *1.6*	139.5 ± *3.5*	4.24 ± *0.11*	0.66 ± *0.02*
	LAG-1 **	43°20'01.9"N 2°22'40.1"E	04/19	873 ± *22*	1.29 ± *0.03*	21.1 ± *0.5*	77.1 ± *1.9*	126.1 ± *3.2*	4.01 ± *0.10*	0.10 ± *0.00*
Russec	RAI-1	43°17'13.5"N 2°23'27.9"E	01/19	171 ± *4*	0.32 ± *0.01*	7.6 ± *0.2*	44.6 ± *1.1*	29.7 ± *0.7*	2.49 ± *0.06*	0.29 ± *0.01*
	RAI-2	43°17'13.5"N 2°23'27.9"E	01/19	279 ± *7*	0.52 ± *0.01*	13.4 ± *0.3*	45.2 ± *1.1*	71.4 ± *1.8*	3.03 ± *0.08*	0.59 ± *0.01*
	RAI-3	43°17'13.5"N 2°23'27.9"E	01/19	255 ± *6*	0.59 ± *0.01*	9.1 ± *0.2*	48.2 ± *1.2*	50.6 ± *1.3*	2.21 ± *0.06*	0.44 ± *0.01*
	RAI-4	43°17'13.5"N 2°23'27.9"E	01/19	161 ± *4*	0.23 ± *0.01*	9.3 ± *0.2*	50.4 ± *1.3*	28.5 ± *0.7*	2.93 ± *0.07*	0.31 ± *0.01*
	RAI-5	43°17'13.5"N 2°23'27.9"E	01/19	161 ± *4*	0.28 ± *0.01*	7.0 ± *0.2*	30.4 ± *0.8*	26.1 ± *0.7*	1.86 ± *0.05*	0.31 ± *0.01*
	SLT-1	43°16'54.0"N 2°23'31.0"E	11/18	151 ± *4*	0.25 ± *0.01*	6.7 ± *0.2*	37.9 ± *0.9*	28.9 ± *0.7*	2.15 ± *0.05*	0.30 ± *0.01*
	SLT-2	43°16'54.0"N 2°23'31.0"E	11/18	403 ± *10*	0.61 ± *0.02*	12.5 ± *0.3*	49.9 ± *1.2*	100.4 ± *2.5*	2.77 ± *0.07*	0.57 ± *0.01*
	SLT-3	43°16'54.0"N 2°23'31.0"E	01/19	246 ± *6*	0.34 ± *0.01*	8.7 ± *0.2*	41.4 ± *1.0*	42.2 ± *1.1*	2.19 ± *0.05*	0.36 ± *0.01*
	SLT-4	43°16'54.0"N 2°23'31.0"E	01/19	249 ± *6*	0.38 ± *0.01*	9.3 ± *0.2*	38.6 ± *1.0*	47.3 ± *1.2*	2.40 ± *0.06*	0.38 ± *0.01*
	SLT-5	43°16'54.0"N 2°23'31.0"E	01/19	203 ± *5*	0.46 ± *0.01*	10.2 ± *0.3*	61.2 ± *1.5*	36.2 ± *0.9*	3.12 ± *0.08*	0.42 ± *0.01*
	SLT-6	43°16'54.0"N 2°23'31.0"E	01/19	274 ± *7*	0.50 ± *0.01*	9.8 ± *0.2*	33.6 ± *0.8*	75.6 ± *1.9*	1.90 ± *0.05*	0.41 ± *0.01*
	SLT-7	43°16'54.0"N 2°23'31.0"E	04/19	341 ± *9*	0.51 ± *0.01*	12.5 ± *0.3*	49.4 ± *1.2*	62.6 ± *1.6*	2.65 ± *0.07*	0.54 ± *0.01*
	ANG-1 **	43°16'36.6"N 2°23'58.2"E	11/18	554 ± *14*	0.70 ± *0.02*	16.9 ± *0.4*	64.2 ± *1.6*	93.8 ± *2.3*	3.38 ± *0.08*	0.77 ± *0.02*
	ANG-2 **	43°16'40.3"N 2°23'50.3"E	01/19	470 ± *12*	0.59 ± *0.01*	16.2 ± *0.4*	62.5 ± *1.6*	88.4 ± *2.2*	3.49 ± *0.09*	0.79 ± *0.02*
	ANG-3 **	43°16'40.3"N 2°23'52.1"E	01/19	631 ± *16*	0.67 ± *0.02*	21.0 ± *0.5*	83.1 ± *2.1*	107.4 ± *2.7*	4.85 ± *0.12*	0.97 ± *0.02*
	ANG-4 **	43°16'40.3"N 2°23'50.3"E	01/19	143 ± *4*	0.41 ± *0.01*	9.2 ± *0.2*	38.6 ± *1.0*	67.3 ± *1.7*	2.38 ± *0.06*	0.41 ± *0.01*

* precipitates
** flood sediments

Table 2 continued

Stream	Sample	Ni	Pb	Sb	Ti ‰	U	V	Zn
Orbiel	MIR-1	4.2 ± *0.1*	17.3 ± *0.4*	0.02 ± *0.00*	0.45 ± *0.01*	0.64 ± *0.02*	14.6 ± *0.4*	66.8 ± *1.7*
	MAS-1	29.6 ± *0.7*	27.9 ± *0.7*	0.24 ± *0.01*	2.00 ± *0.05*	1.95 ± *0.05*	96.8 ± *2.4*	92.9 ± *2.3*
	LAS-1	33.7 ± *0.8*	27.5 ± *0.7*	1.66 ± *0.04*	2.11 ± *0.05*	2.18 ± *0.05*	101.0 ± *2.5*	77.1 ± *1.9*
	ART-1	35.3 ± *0.9*	43.8 ± *1.1*	1.60 ± *0.04*	1.35 ± *0.03*	1.85 ± *0.05*	93.0 ± *2.3*	98.5 ± *2.5*
	LIM-1	32.2 ± *0.8*	42.3 ± *1.1*	2.28 ± *0.06*	1.72 ± *0.04*	2.02 ± *0.05*	106.2 ± *2.7*	125.0 ± *3.1*
	LIM-2	30.7 ± *0.8*	41.1 ± *1.0*	2.70 ± *0.07*	1.95 ± *0.05*	1.93 ± *0.05*	90.2 ± *2.3*	104.0 ± *2.6*
	WTS-1	30.2 ± *0.8*	43.0 ± *1.1*	1.68 ± *0.04*	4.00 ± *0.10*	2.25 ± *0.06*	91.2 ± *2.3*	114.6 ± *2.9*
	WTS-2	24.4 ± *0.6*	43.4 ± *1.1*	7.07 ± *0.18*	1.86 ± *0.05*	1.69 ± *0.04*	85.7 ± *2.1*	90.1 ± *2.3*
	WTS-3	24.1 ± *0.6*	22.9 ± *0.6*	1.36 ± *0.03*	2.08 ± *0.05*	1.82 ± *0.05*	87.9 ± *2.2*	92.1 ± *2.3*
	WTS-4	26.5 ± *0.7*	73.9 ± *1.8*	2.70 ± *0.07*	4.19 ± *0.10*	1.70 ± *0.04*	76.2 ± *1.9*	94.2 ± *2.4*
	WTS-6	26.1 *0.7*	717.9 *17.9*	1.47 *0.04*	5.30 *0.13*	1.97 *0.05*	85.6 *2.1*	97.6 *2.4*
	WTS-7	40.3 *1.0*	832.5 *20.8*	2.44 *0.06*	5.23 *0.13*	3.32 *0.08*	91.3 *2.3*	142.3 *3.6*
	WTS-8	25.9 *0.6*	105.1 *2.6*	3.32 *0.08*	1.88 *0.05*	1.40 *0.03*	63.6 *1.6*	93.5 *2.3*
	WTS-9	23.6 *0.6*	322.2 *8.1*	8.03 *0.20*	4.06 *0.10*	1.85 *0.05*	67.2 *1.7*	94.1 *2.4*
	GUE-1	32.9 ± *0.8*	55.3 ± *1.4*	2.59 ± *0.06*	1.95 ± *0.05*	2.06 ± *0.05*	97.3 ± *2.4*	129.2 ± *3.2*
	GUE-2 *	9.7 ± *0.2*	22.8 ± *0.6*	2.51 ± *0.06*	0.35 ± *0.01*	0.88 ± *0.02*	15.3 ± *0.4*	120.1 ± *3.0*
	GUE-3 *	30.1 ± *0.8*	96.6 ± *2.4*	3.78 ± *0.09*	1.46 ± *0.04*	2.98 ± *0.07*	84.5 ± *2.1*	120.2 ± *3.0*
	GUE-4	32.5 ± *0.8*	103.6 ± *2.6*	3.62 ± *0.09*	1.77 ± *0.04*	2.53 ± *0.06*	85.1 ± *2.1*	110.0 ± *2.8*
	GUE-5	39.9 ± *1.0*	20.7 ± *0.5*	0.92 ± *0.02*	2.63 ± *0.07*	2.32 ± *0.06*	120.4 ± *3.0*	100.1 ± *2.5*
	GUE-6	61.1 ± *1.5*	157.0 ± *3.9*	5.11 ± *0.13*	1.58 ± *0.04*	3.51 ± *0.09*	152.7 ± *3.8*	204.4 ± *5.1*
	GUE-7	26.9 ± *0.7*	65.6 ± *1.6*	1.97 ± *0.05*	1.75 ± *0.04*	1.84 ± *0.05*	66.6 ± *1.7*	93.6 ± *2.3*
	GUE-8	34.2 ± *0.9*	67.9 ± *1.7*	2.46 ± *0.06*	2.22 ± *0.06*	2.24 ± *0.06*	98.3 ± *2.5*	120.5 ± *3.0*
Grésillou	NAU-1	49.8 ± *1.2*	24.5 ± *0.6*	0.83 ± *0.02*	1.38 ± *0.03*	2.99 ± *0.07*	126.6 ± *3.2*	110.9 ± *2.8*
	NAU-2	51.5 ± *1.3*	30.9 ± *0.8*	0.70 ± *0.02*	2.35 ± *0.06*	3.10 ± *0.08*	135.3 ± *3.4*	108.0 ± *2.7*
	NAU-3	30.6 ± *0.8*	103.8 ± *2.6*	3.31 ± *0.08*	0.96 ± *0.02*	2.19 ± *0.05*	89.5 ± *2.2*	122.4 ± *3.1*
	NAU-4	39.5 ± *1.0*	20.1 ± *0.5*	0.67 ± *0.02*	2.19 ± *0.05*	2.20 ± *0.06*	120.9 ± *3.0*	91.2 ± *2.3*
	NAD-1	41.5 ± *1.0*	41.5 ± *1.0*	4.46 ± *0.11*	1.35 ± *0.03*	2.16 ± *0.05*	108.7 ± *2.7*	156.9 ± *3.9*
	NAD-2	45.6 ± *1.1*	24.7 ± *0.6*	1.46 ± *0.04*	2.81 ± *0.07*	2.69 ± *0.07*	113.8 ± *2.8*	112.0 ± *2.8*
	NAD-3	42.5 ± *1.1*	96.0 ± *2.4*	15.57 ± *0.39*	0.57 ± *0.01*	3.37 ± *0.08*	136.3 ± *3.4*	96.8 ± *2.4*
	NAD-4	46.2 ± *1.2*	202.3 ± *5.1*	36.17 ± *0.90*	1.13 ± *0.03*	2.22 ± *0.06*	91.7 ± *2.3*	116.2 ± *2.9*
	LAG-1 **	52.2 ± *1.3*	74.0 ± *1.8*	3.97 ± *0.10*	1.45 ± *0.04*	2.60 ± *0.07*	113.8 ± *2.8*	185.1 ± *4.6*
Russec	RAI-1	20.5 ± *0.5*	40.8 ± *1.0*	2.50 ± *0.06*	1.07 ± *0.03*	1.79 ± *0.04*	67.3 ± *1.7*	49.8 ± *1.2*
	RAI-2	30.8 ± *0.8*	37.9 ± *0.9*	1.90 ± *0.05*	1.49 ± *0.04*	1.98 ± *0.05*	70.7 ± *1.8*	74.6 ± *1.9*
	RAI-3	22.0 ± *0.6*	34.0 ± *0.8*	2.05 ± *0.05*	1.51 ± *0.04*	1.82 ± *0.05*	69.0 ± *1.7*	51.3 ± *1.3*
	RAI-4	23.2 ± *0.6*	32.8 ± *0.8*	1.61 ± *0.04*	1.99 ± *0.05*	2.07 ± *0.05*	68.9 ± *1.7*	48.5 ± *1.2*
	RAI-5	15.9 ± *0.4*	28.1 ± *0.7*	1.44 ± *0.04*	1.66 ± *0.04*	1.76 ± *0.04*	45.5 ± *1.1*	36.9 ± *0.9*
	SLT-1	17.4 ± *0.4*	52.7 ± *1.3*	2.05 ± *0.05*	0.87 ± *0.02*	1.17 ± *0.03*	56.2 ± *1.4*	56.5 ± *1.4*
	SLT-2	27.9 ± *0.7*	41.0 ± *1.0*	2.51 ± *0.06*	1.61 ± *0.04*	1.87 ± *0.05*	70.3 ± *1.8*	83.8 ± *2.1*
	SLT-3	20.9 ± *0.5*	32.6 ± *0.8*	2.01 ± *0.05*	1.66 ± *0.04*	1.89 ± *0.05*	60.1 ± *1.5*	54.2 ± *1.4*
	SLT-4	23.7 ± *0.6*	35.8 ± *0.9*	2.03 ± *0.05*	1.64 ± *0.04*	1.94 ± *0.05*	58.2 ± *1.5*	53.0 ± *1.3*
	SLT-5	25.7 ± *0.6*	48.3 ± *1.2*	2.42 ± *0.06*	1.41 ± *0.04*	2.22 ± *0.06*	86.0 ± *2.1*	65.2 ± *1.6*
	SLT-6	22.9 ± *0.6*	40.8 ± *1.0*	2.03 ± *0.05*	0.92 ± *0.02*	1.28 ± *0.03*	50.2 ± *1.3*	57.6 ± *1.4*
	SLT-7	28.4 ± *0.7*	37.0 ± *0.9*	2.09 ± *0.05*	1.80 ± *0.05*	2.08 ± *0.05*	70.6 ± *1.8*	64.6 ± *1.6*
	ANG-1 **	34.6 ± *0.9*	41.2 ± *1.0*	3.03 ± *0.08*	1.92 ± *0.05*	2.35 ± *0.06*	92.9 ± *2.3*	102.6 ± *2.6*
	ANG-2 **	38.3 ± *1.0*	41.0 ± *1.0*	2.43 ± *0.06*	1.76 ± *0.04*	2.68 ± *0.07*	91.5 ± *2.3*	72.9 ± *1.8*
	ANG-3 **	50.0 ± *1.2*	54.1 ± *1.4*	3.43 ± *0.09*	2.60 ± *0.07*	3.74 ± *0.09*	127.2 ± *3.2*	101.9 ± *2.5*
	ANG-4 **	24.8 ± *0.6*	35.6 ± *0.9*	1.62 ± *0.04*	1.57 ± *0.04*	1.80 ± *0.05*	62.4 ± *1.6*	63.3 ± *1.6*

* precipitates
** flood sediments

Table 3 : Pedo-geochemical background in the Orbiel valley.

Element	Unit	Pedo-geochemical background (Orbiel valley)	Baselines	
			France [1]	Europe [2]
As	$mg.kg^{-1}$	44 ± 12	12	6
Cd	$mg.kg^{-1}$	0.18 ± 0.06	0.11	0.09
Co	$mg.kg^{-1}$	13 ± 10	10	9
Cr	$mg.kg^{-1}$	84 ± 16	51	62
Cu	$mg.kg^{-1}$	38 ± 16	12	14
Fe	%	3.90 ± 1.37	2.49	3.75
Mn	%	0.07 ± 0.03	0.05	0.06
Ni	$mg.kg^{-1}$	28 ± 18	21	22
Pb	$mg.kg^{-1}$	38 ± 21	23	17
Sb	$mg.kg^{-1}$	0.9 ± 1.2	-	0.5
Ti	%	0.44 ± 0.09	0.42	0.57
U	$mg.kg^{-1}$	2.6 ± 0.3	-	2.0
V	$mg.kg^{-1}$	126 ± 16	-	63
Zn	$mg.kg^{-1}$	92 ± 44	59	47

Mean concentrations in soils (baselines) are reported at the French and European scales are reported for comparison : [1] **Saby et al. (2019)** ; [2] **Salimen et al. (2005)**.

Table 4: Geo-accumulation index have been calculated according to the formula proposed by Müller (1969)

	As	Cd	Co	Cr	Cu	Fe %	Mn ‰	Ni	Pb	Sb	Ti ‰	U	V	Zn
MIR-1	-1.9	-0.3	-1.9	0.3	-3.3	-1.9	-1.6	-2.2	0.3	-4.8	0.6	-1.4	-2.5	0.1
MAS-1	0.4	1.2	0.2	1.0	0.2	0.4	-0.1	0.7	1.0	-1.3	2.8	0.2	0.2	0.6
LAS-1	0.6	1.7	0.3	1.0	0.8	0.3	0.1	0.9	1.0	1.5	2.8	0.3	0.3	0.3
ART-1	2.9	2.3	0.7	1.6	0.8	0.2	1.1	0.9	1.6	1.4	2.2	0.1	0.1	0.7
LIM-1	3.0	1.7	0.3	1.6	1.0	0.7	0.1	0.8	1.6	1.9	2.6	0.2	0.3	1.0
LIM-2	2.2	1.8	0.3	1.6	1.1	0.4	0.3	0.7	1.6	2.2	2.7	0.2	0.1	0.8
WTS-1	2.2	1.5	0.1	1.6	0.8	0.5	0.5	0.7	1.6	1.5	3.8	0.4	0.1	0.9
WTS-2	1.5	1.2	-0.1	1.6	0.4	0.0	-0.1	0.4	1.6	3.6	2.7	0.0	0.0	0.6
WTS-3	2.5	1.8	-0.2	0.7	0.6	0.1	-0.5	0.4	0.7	1.2	2.8	0.1	0.1	0.6
WTS-4	1.7	0.9	0.0	2.4	0.0	0.1	-0.3	0.5	2.4	2.2	3.8	0.0	-0.1	0.6
WTS-6	2.5	1.5	-0.1	5.7	0.5	0.2	0.2	0.5	5.7	1.3	4.2	0.2	0.0	0.7
WTS-7	2.8	2.3	0.7	5.9	1.7	0.7	1.1	1.1	5.9	2.0	4.2	0.9	0.1	1.2
WTS-8	4.1	2.3	-0.1	2.9	0.7	0.5	0.2	0.5	2.9	2.5	2.7	-0.3	-0.4	0.6
WTS-9	3.8	1.4	-0.3	4.5	1.3	0.1	-0.2	0.3	4.5	3.7	3.8	0.1	-0.3	0.6
GUE-1	3.1	2.5	0.4	2.0	1.1	0.6	0.6	0.8	2.0	2.1	2.7	0.3	0.2	1.1
GUE-2 *	-0.1	4.4	-0.9	0.7	1.5	2.4	1.1	-0.9	0.7	2.1	0.2	-1.0	-2.5	1.0
GUE-3 *	-1.0	3.9	0.6	2.8	1.4	2.1	2.0	0.7	2.8	2.7	2.3	0.8	0.0	1.0
GUE-4	3.9	2.4	0.4	2.9	2.0	0.5	0.7	0.8	2.9	2.6	2.6	0.5	0.0	0.8
GUE-5	2.0	1.2	0.7	0.6	0.8	0.8	0.7	1.1	0.6	0.6	3.2	0.4	0.5	0.7
GUE-6	3.8	3.0	1.3	3.5	1.7	1.4	1.2	1.7	3.5	3.1	2.4	1.0	0.9	1.7
GUE-7	-4.4	2.6	0.2	2.2	1.0	0.4	0.7	0.5	2.2	1.7	2.6	0.1	-0.3	0.6
GUE-8	4.1	2.6	0.4	2.3	1.4	0.7	0.6	0.9	2.3	2.0	2.9	0.4	0.2	1.0
NAU-1	2.0	1.1	1.0	0.8	0.9	0.7	0.4	1.4	0.8	0.5	2.2	0.8	0.6	0.9
NAU-2	2.7	0.8	1.0	1.1	1.2	0.8	0.5	1.5	1.1	0.2	3.0	0.8	0.7	0.8
NAU-3	3.3	2.6	0.4	2.9	1.5	0.8	0.5	0.7	2.9	2.5	1.7	0.3	0.1	1.0
NAU-4	2.1	1.7	0.8	0.5	0.6	0.6	0.6	1.1	0.5	0.2	2.9	0.3	0.5	0.6
NAD-1	-4.3	2.9	0.7	1.6	4.0	0.9	0.9	1.2	1.6	2.9	2.2	0.3	0.4	1.4
NAD-2	3.6	1.2	0.8	0.8	1.3	0.8	0.9	1.3	0.8	1.3	3.3	0.6	0.4	0.9
NAD-3	-2.2	2.1	0.5	2.8	2.2	1.9	1.1	1.2	2.8	4.7	1.0	1.0	0.7	0.7
NAD-4	-3.7	3.8	1.3	3.9	2.5	0.7	0.5	1.3	3.9	5.9	1.9	0.4	0.1	0.9
LAG-1 **	4.9	3.4	1.3	2.4	2.3	0.6	-2.2	1.5	2.4	2.7	2.3	0.6	0.4	1.6
RAI-1	2.5	1.4	-0.2	1.5	0.2	-0.1	-0.7	0.1	1.5	2.1	1.9	0.0	-0.3	-0.3
RAI-2	3.2	2.1	0.6	1.4	1.5	0.2	0.3	0.7	1.4	1.7	2.3	0.2	-0.2	0.3
RAI-3	3.1	2.3	0.1	1.3	1.0	-0.2	-0.1	0.2	1.3	1.8	2.4	0.1	-0.3	-0.3
RAI-4	2.5	0.9	0.1	1.2	0.2	0.2	-0.6	0.3	1.2	1.4	2.8	0.3	-0.3	-0.3
RAI-5	2.5	1.2	-0.3	1.0	0.0	-0.5	-0.6	-0.2	1.0	1.3	2.5	0.0	-0.9	-0.7
SLT-1	2.4	1.1	-0.4	1.9	0.2	-0.3	-0.6	-0.1	1.9	1.8	1.6	-0.6	-0.6	-0.1
SLT-2	3.8	2.4	0.5	1.5	2.0	0.1	0.3	0.6	1.5	2.1	2.5	0.1	-0.3	0.4
SLT-3	3.1	1.5	0.0	1.2	0.7	-0.2	-0.4	0.2	1.2	1.7	2.5	0.1	-0.5	-0.2
SLT-4	3.1	1.7	0.1	1.4	0.9	-0.1	-0.3	0.3	1.4	1.8	2.5	0.2	-0.5	-0.2
SLT-5	2.8	1.9	0.2	1.8	0.5	0.3	-0.1	0.5	1.8	2.0	2.3	0.4	0.0	0.1
SLT-6	3.2	2.1	0.2	1.5	1.6	-0.5	-0.2	0.3	1.5	1.8	1.6	-0.4	-0.7	-0.1
SLT-7	3.5	2.1	0.5	1.4	1.3	0.0	0.2	0.6	1.4	1.8	2.6	0.3	-0.3	0.1
ANG-1 **	4.2	2.6	1.0	1.6	1.9	0.4	0.7	0.9	1.6	2.3	2.7	0.4	0.1	0.7
ANG-2 **	4.0	2.3	0.9	1.5	1.8	0.4	0.8	1.0	1.5	2.0	2.6	0.6	0.1	0.2
ANG-3 **	4.4	2.5	1.3	1.9	2.1	0.9	1.1	1.4	1.9	2.5	3.1	1.1	0.6	0.7
ANG-4 **	2.3	1.8	0.1	1.3	1.4	-0.1	-0.2	0.4	1.3	1.4	2.4	0.1	-0.4	0.0

	Value	Class	
	0	0	uncontaminated
	0 et 1	1	uncontaminated to moderately contaminated
	1 et 2	2	moderately contaminated
	2 et 3	3	moderately to strongly contaminated
	3 et 4	4	strongly contaminated
	4 et 5	5	strongly to extremely contaminated
	> 5	6	extremely contaminated